Snowman particles with microspheres and polymers

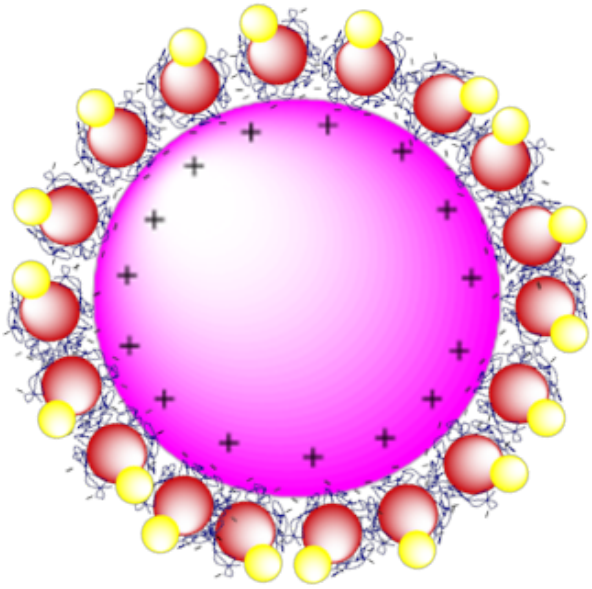

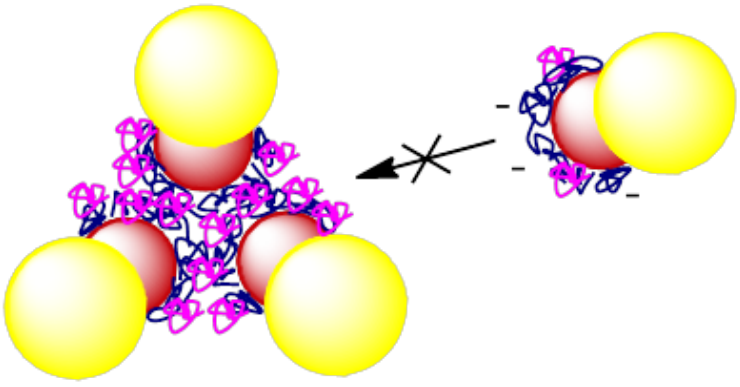

Ellen G. Heuven

Universiteit Utrecht

Masterthesis

Aggregation behavior of snowman-like particles with oppositely charged large microspheres and polymers

Author:
Ellen G. Heuven

Supervisors:
Yong Guo and
Prof. Willem K. Kegel

August 17, 2017

Abstract

Recently Evers et al. [1] have shown that snowman particles assemble into hollow virus-like capsules in the absence of template. In this thesis I will show the aggregation behavior of the snowman particles in the presence of oppositely charged large template. Also the aggregation behavior of snowman particles with oppositely charged polymer (acts as extremely small template) was studied. Three types of snowman particles with a protrusion larger, slightly larger and slightly smaller than the seed particle were synthesized. The coverage of the microspheres by each of the snowman particles was influenced by the ionic strength, the pH and the size of the protrusion, but the size of the microsphere had little influence. With oppositely charged polymer the snowman particles formed random large clusters, except for he snowman particles with the largest protrusion. This behavior of snowman particles with oppositely charged templates might provide some insight in the formation process of virus shells.

Contents

Chapter 1

Introduction

Simple building blocks can assemble into ordered or disordered structures. The clotting of blood, the coagulation of egg white, the Alzheimer disease and Parkinson disease are examples of the formation of disordered structures in nature. [2, 3, 4] When the building blocks assemble into ordered structures without human intervention this is called self-assembly. [5] A lot of different structures are formed by self -assembly, for example crystals, soap bubbles, lipid bilayers, virus capsids and cytoskeletons of cells. [5, 6, 7]

Some of these self-assembled structures are too small to be observed with an optical microscope. In order to study the self-assembly of these structures, for example the assembly of virus proteins around viral DNA (figure 1.1), [7] a model system is required. Like the virus proteins and DNA, colloids are small enough to exhibit Brownian motion. [8] However in contrast to the virus counterparts, colloids are big enough to be visible with an optical microscope, [9] which makes them suitable as a model system for the self-assembly of virus capsids.

The adsorption of small particles on bigger ones can be used as model system for this self-assembly. The adsorption has been studied in the case of oppositely charged spheres, for both positive small with negative big spheres and negative small on positive big spheres. [10, 11, 12] Instead of the isotropic spheres, anisotropic particles such as snowman particles are a better model for proteins, since they have domains with different properties like proteins have. [13] Evers et al. showed that snowman particles can form hollow virus-like shells (figure 1.2). [1] However, a system of these snowman particles with oppositely charged big spheres has not yet been studied. We expect that a virus-like shell consisting of snowman particles can be formed around the big sphere, like a proteins shell formed around DNA.

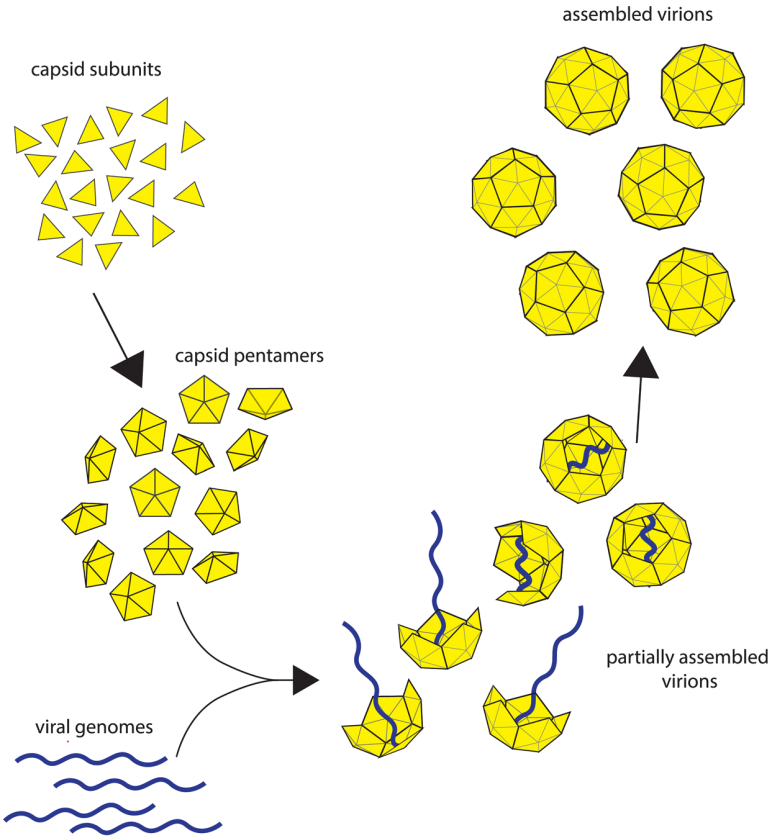

Figure 1.1: The self-assembly of virus proteins and viral DNA to filled shells. [7]

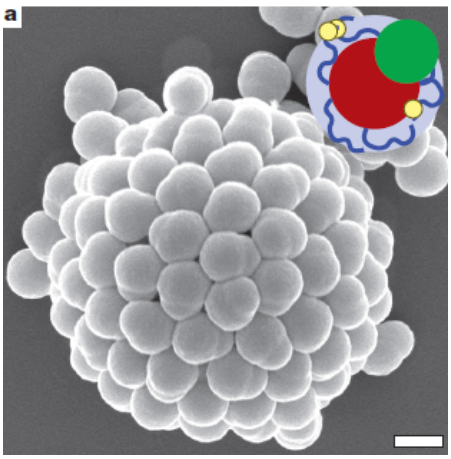

Figure 1.2: A hollow shell of snowman particles that resembles the shell of a virus. [1]

In this thesis a model system of snowman particles with oppositely charged larger spheres for the formation of protein shells around viral DNA is made. In this system, the negatively charged snowman particles are a model for the proteins and the positively charged microspheres are a model for the viral DNA (figure 1.3). The coverage and the orientation of the snowman particles on the microspheres are studied under different conditions. These conditions are the pH and ionic strength of the solution, the size of the snowman particles and the microspheres.

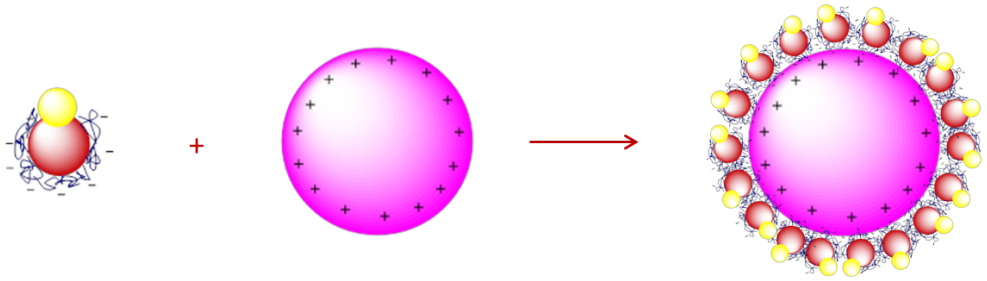

Figure 1.3: An illustration of the adsorption of snowman particles on a bigger positively charged sphere.

Another interesting self-assembly system is the formation of finite-sized clusters, for example micelles and colloidal molecules. [14, 15] This formation has been modelled a lot experimentally and with computer simulations with patchy particles, however to make these particles multiple complicated synthesis and functionalization steps are required. [15, 16, 17] An easier way to make these clusters could be with relatively easy to make snowman-like particles with oppositely charged polymers (figure 1.4).

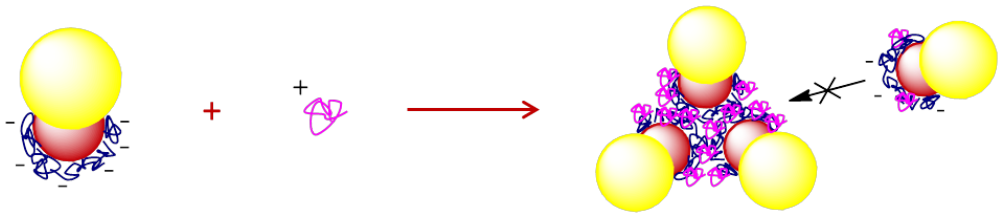

Figure 1.4: An illustration of the aggregation of snowman particles with oppositely charged polymers.

In this thesis the aggregation behavior of snowman particles in the presence of oppositely charged polymer is studied. The size of the protrusion and the amount of polymer is varied, in order to see if the protrusion sterically stabilizes the aggregation which results in finite-sized clusters.

Chapter 2

Theory

2.1 Dispersion polymerization

The big positively charged particles are made by stabilizer-free dispersion polymerization. Conventional dispersion polymerization is the polymerization of monomer or co-monomers dissolved in a solvent or solvent mixture in the presence of a suitable steric stabilizer. With stabilizer free dispersion polymerization no steric stabilizer is used, a positively charged co-monomer METMAC ((2-(methacryloyloxy) ethyl) trimethylammonium chloride, figure 2.1a) is copolymerized with styrene (figure 2.1b). Due to the charge and hydrophilicity of METMAC, the segments that are rich in co-monomer reside at the surface of the formed particles. These charged segments cause the electrostatic repulsion between the particles which stabilizes the particles. [18]

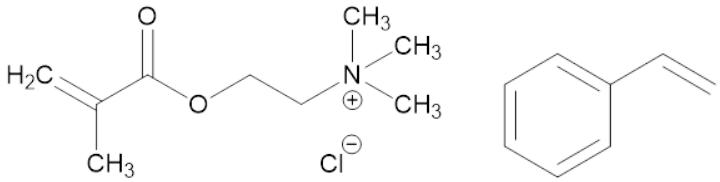

(a) METMAC (b) Styrene

Figure 2.1: The structures of the dispersion polymerization chemicals.

Before polymerization, styrene, METMAC and the initiator are dissolved in the solvent, this solution is homogeneous and transparent (figure 2.2a). By heating the solution, the initiator produces radicals that initiate the polymerization. When styrene and METMAC start polymerizing, random copolymers are formed (figure

2.2b). When these copolymers reach the critical chain length the copolymers cannot be dissolved anymore, so they precipitate, entangle, and coalesce to form the nuclei (figure 2.2c). The nuclei grow by adsorbing copolymers in the solvent or by adsorption of monomers and subsequent polymerization. Therefore positively charged polystyrene microspheres are formed (figure 2.2d). [18]

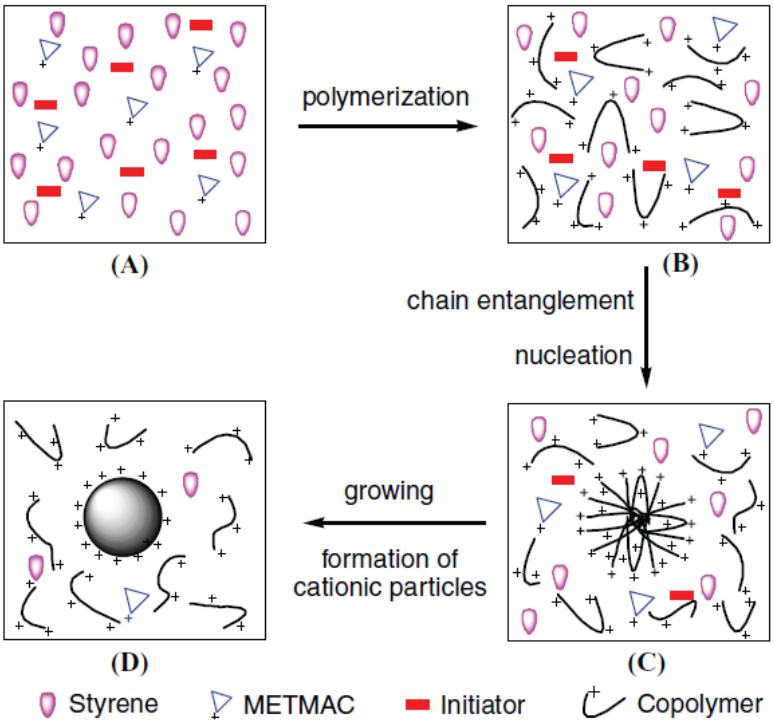

Figure 2.2: Schematic illustrations of the formation of positively charged polystyrene microspheres in a methanol / water system. [18]

2.2 Emulsifier-free emulsion polymerization

Emulsifier-free emulsion co-polymerization of styrene with negatively charged co-monomer was used to make negatively charged spherical seed particles. These seed particles will later function as body of the snowman particles. Before the polymerization, styrene, acrylic acid (figure 2.3a), DVB (crosslinker, figure 2.3b) and initiator are mixed in water to form an emulsion. By heating the emulsion, the initiator produces radicals that initiate the polymerization. When styrene, crosslinker and acrylic acid start polymerizing, oligomer radicals are formed. When these oligomer radicals reach a critical length, they precipitate and agglomerate

to form nuclei. These nuclei grow into particles with a core / shell structure, which is caused by the different interactions of the monomers with water. The core consists mainly of hydrophobic crosslinked polystyrene and the shell of hydrophilic polyacrylic acid. This negatively charged shell stabilizes the particles, because of the hydrophilicity and the electrostatic repulsion. [19]

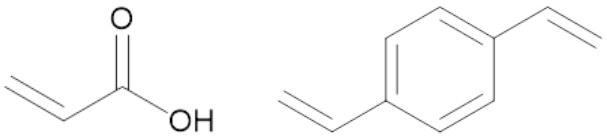

(a) Acrylic acid (b) DVB

Figure 2.3: The structures of the emulsion polymerization chemicals.

2.3 Protrusion formation

Snowman particles are made by growing a protrusion on the seed particle and then polymerizing this protrusion. The hydrophilic former seed particle is called the "body" and the hydrophobic protrusion is called the "head" of the snowman particle. The protrusion is made by swelling and heating the seed particle, then the protrusion is polymerized and the snowman particle is made (figure 2.4). When styrene and crosslinker are added to the crosslinked spherical particle, the monomers diffuse into it which causes the crosslinked particle to swell. This swelling is a balance between the free energy of mixing of the monomer with the polymer, the elastic energy of stretching the chains within the crosslinked seed particles and the surface tension of the particle/water interface. When the temperature is increased, the elastic force also increases. This decreases the equilibrium swelling ratio, which causes monomers to be expelled from the crosslinked particle. These expelled monomers bulge out of the particle and form a protrusion. The size of this protrusion is dependent on how much monomers are added per crosslinked particle. When the emulsion is heated after the addition of initiator, the protrusion is polymerized and a snowman particle is made. [20, 21]

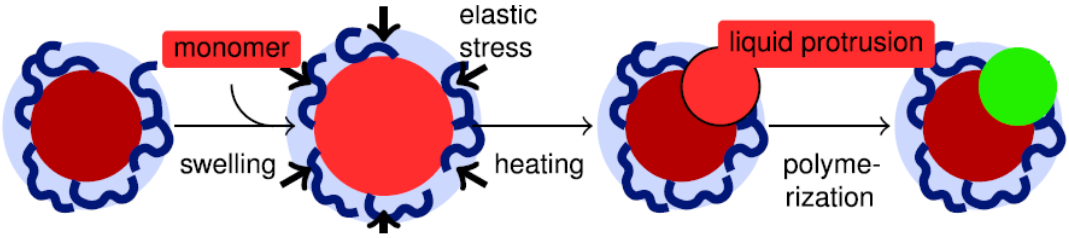

Figure 2.4: A scheme of the formation of the protrusion on the seed particle by swelling, heating and polymerization. [1]

2.4 Interactions of snowman particles

2.4.1 In water

Two types of interactions have to be taken into account by the adsorption of small isotropic charged particles on larger oppositely charged particles. One set of interactions is between the small particles and the bigger particle, these are the main adsorbing forces. The other set of interactions are the interactions between the adsorbed particles. These sets of interactions consist of electrostatic interactions and van der Waals interactions. [10]

Anisotropic snowman particles have a bit different interactions than isotropic particles with the bigger oppositely charged particles (figure 2.5). Since the seed of the snowman particles is similar to an isotropic particle, the electrostatic interactions are the same. However the snowman particles have a hydrophobic protrusion, which increases the radius and the van der Waals interactions. These different domains of the snowman particles cause to directional interactions due to the different interactions. These directional interactions combined with the increased attraction can give rise to different adsorption behavior.

Instead of large particles, polymers could also be added as oppositely charged templates for the snowman particles. In contrast to the large particles, the polymers are smaller than the snowman particles, which results in different interactions. If the polymer adsorbs on a seed particle, this particle becomes partially positive charged. This positive patch on the particle is attracted to negatively charged patches on the particles, which causes the particles aggregate. So if the amount of polymer is increased, the amount of positive patches increase and the stability of the particles decrease. However if a lot of polymers adsorb on the particles, there are more positive than negative patches and the stability increases again due to charge inversion. [22]

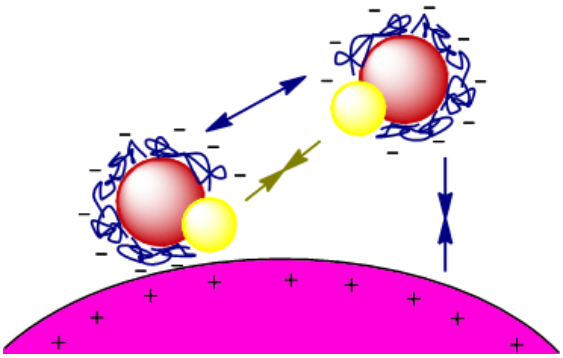

Figure 2.5: In yellow is the hydrophobic attraction of the head indicated and the electrostatic interactions of body are indicated in blue. These electrostatic interactions are the repulsion between the snowman particles and the attraction to the oppositely charged microsphere.

2.4.2 In salt solution

When the salt concentration is increased, the Debye length (κ^{-1}) is decreased (equation 2.1, 25 °C water with 1:1 electolyte: equation 2.2).

$$\kappa^{-1} = \sqrt{\frac{\varepsilon_r \varepsilon_0 k_\mathrm{B} T}{2 N_\mathrm{A} e^2 I}} \tag{2.1}$$

$$\kappa^{-1}(\mathrm{nm}) = \frac{3.04}{\sqrt{I(\mathrm{M})}} \tag{2.2}$$

This results in a decrease of the electrostatic repulsion and adsorption, but the hydrophobic attraction of the protrusion does not decrease with a decrease in Debye length. This causes a change from net repulsion to net attraction between the microsphere and snowman particles when the the salt concentration is increased. [10]

2.4.3 At low pH

The p*K*a of AA is 4.5, which means that below this pH the acid groups get protonated and the charge of the particle decreases. [23] When the pH values are a lot lower than the p*K*a and higher than 2, most the AA groups are protonated and only the charged groups of the initiator (p*K*a = 2) are left. This results into a very low charge and hydrophobic hairs, which causes them to collapse on the particle. This decrease of charge also results in a decrease in the stability of the snowman particles.

Chapter 3

Methods

3.1 Chemicals

The water used throughout all of the experiments was purified using a milli-Q purification system. See table 3.1 for the purity of the other chemicals and where they are purcased.

Table 3.1: The chemicals used in the experiments.

Name chemical and purity	Abbreviation	Purchased at
Acrylic acid 99 %	AA	Sigma-Aldrich
Divinylbenzene (mixture of isomers) 55 %, tech. grade	DVB	Sigma-Aldrich
N-(3-dimethylaminopropyl)-N'-ethylcarbodiimine hydrochloride $\geq$ 98.0 %	EDC	Sigma-Aldrich
Fluoresceinamine $\geq$ 75 %	FIA	Sigma-Aldrich
2-(N-Morpholino) ethanesulphonic acid $\geq$ 99 %	MES	Sigma-Aldrich
(2-(methacryloyloxy) ethyl) trimethylammonium chloride 80 % in H_2O	METMAC	Sigma-Aldrich
Sodium phosphate dibasic $\geq$ 99 %	Na_2HPO_4	Sigma-Aldrich
Sodium phosphate monobasic dehydrate $\geq$ 99 %	$NaH_2PO_4 \cdot 2\,H_2O$	Sigma-Aldrich
Polyethylenimine, branched (Mw = 25 kDa) $\geq$ 99 %	bPEI	Sigma-Aldrich

Continued on next page

Table 3.1 – Continued

Name chemical and purity	Abbreviation	Purchased at
Polyethylenimine, linear (Mw = 10 kDa) PDI $\leq$ 1.2	lPEI	Sigma-Aldrich
Styrene 99 %	St	Sigma-Aldrich
2,2'-azobis(2-methyl- propionitrile) 98 %	AIBN	Acros Organics
Potassium chloride $\geq$ 99 %	KCl	Acros Organics
Potassium persulfate $\geq$ 99 % for analysis	KPS	Acros Organics
Ethanol 100 %		Interchema
Hydrochloric acid 36 % to 38 %, chem. pure	HCl	Merck
Hydroquinone $\geq$ 99.5 %, puriss		Riedel-de Haën
Methanol, absolute 99.9 %		Biosolve BV

3.2 Particles synthesis

3.2.1 Synthesis of positively charged large microspheres

The positively charged large microspheres were made by stabilizer free dispersion co-polymerization of styrene with METMAC following Liu et al. [18] 37.5 mL methanol, 12.5 mL water, 90.6 mg AIBN, 123 µL METMAC and 10.0 mL St were added to the dispersion polymerization setup (figure 3.1a). This setup consists of an oil bath with a 100 mL three-neck round-bottom flask. The flask is equipped with a mechanical stirrer, a condenser and a nitrogen gas inlet. The monomer mixture was purged with nitrogen for 30 minutes. While mechanically stirring, the mixture was heated to 75 °C to initiate the polymerization. The reaction was allowed to proceed for 8 hours. The final product was washed with ethanol and water. The washing steps are done by centrifuging the dispersion and then replacing supernatant. The dispersion was washed until the supernatant was colorless. Finally, the product was stored in water.

3.2.2 Synthesis of negatively charged snowman particles

Synthesis of seed particles

The negatively charged seed particles were made by emulsifier free emulsion co-polymerization of St with AA following Evers et al. [1] and Hu et al. [20] 90 mL water, 11 mL St, 55 µL DVB, 0.05 g KPS in 10 mL water and 761 µL AA were

added to the emulsion polymerization setup (figure 3.1b). This setup consists of an oil bath with a 250 mL two-neck round-bottom flask. The flask was constantly stirred under nitrogen flow. After 15 minutes the nitrogen inlet was raised above the liquid level, after another 15 minutes the bath was heated to 70 °C to initiate the polymerization. After 20 hours a white dispersion was obtained, this dispersion was washed three times with water. Finally, the product was stored in water.

Protrusion formation

A protrusion was grown on the seed particles following Evers, [1] however no inhibitor was used. The negatively charged seed particles were swelled, heated to obtain a protrusion and this protrusion was polymerized to form the snowman particles. The solid content (w_s) of the seed particles was brought to 2.9 % g mL^{-1} with water. 5 mL of this diluted dispersion and different amounts of St (table 3.2) where added to the swelling setup (figure 3.1c). This setup consists of long glass bottle with a mechanical stirring bar in an oil bath. The different amounts of St result in different protrusion sizes. The dispersion was stirred for one day at room temperature, subsequently it was put in a 80 °C bath for two hours with continuous stirring. The bottle was removed from the bath to let it cool down and 5 mg AIBN in 250 µL St was added, after this it was put back into the 80 °C bath to initiate the polymerization. After 24 hours the bath was removed and the white dispersion was washed 4x with ethanol and 5x with water. Finally, the product was stored in water.
Sr1.5 and Sr5.5 were also made with this method, however an 500 µL of an aqueous hydroquinone solution (45 mg/50 mL) was added during the addition of AIBN.

Table 3.2: The amounts of added styrene (St) and the corresponding swelling ratios (S) for the protrusion formation.

Sample name	Added St (mL)	S
Sr1	0.16	1.0
Sr2	0.32	2.0
Sr3	0.48	3.0
Sr5	0.81	5.0
Sr7	1.13	7.0
Sr9	1.45	9.0

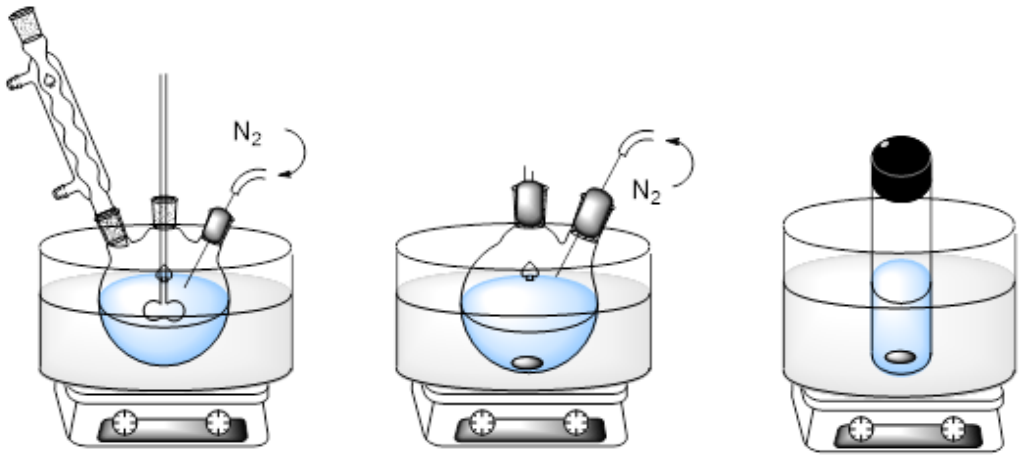

(a) Dispersion polymerization setup

(b) Emulsion polymerization setup

(c) Swelling setup

Figure 3.1: Schemes of the different setups used in the synthesis of the particles.

Functionalization

The functionalization of Sr3 with FIA is preformed following the procedure of Evers et al. [1] A 0.10 M MES buffer and a 0.21 M phosphate buffer (NaH_2PO_4:Na_2HPO_4 = 1:13.7) were made. 1.0 mL of Sr3 (1 % g mL^{-1}) was brought into an Eppendorf tube. After centrifugation, the supernatant was replaced by the EDC/MES solution (6 mM EDC in 0.1 M MES buffer) to activate the AA groups (in order to get a good leaving group). After the dispersion was tumbled for one hour, it was washed once with the MES buffer, twice with water. The sample was dispersed in the FIA/phosphate solution (0.9 mM FIA in 0.2 M phosphate buffer) to covalently bind FIA to the activated AA groups. Aluminium foil was put around the tube and it was placed on the roller-table. After 15 hours the sample was washed again, this was done thrice with the phosphate buffer, once with the MES buffer and ten times with water. Finally, the total volume of the tube was brought with water to 5 mL (w_s = 2 % g mL^{-1}).

3.3 Capsule formation test

In this paragraph the centrifugation and functionalization experiments of snowman particles are preformed following the procedure of Evers et al. [1]

3.3.1 Non-functionalized particles

500 µL of non-functionalized snowman dispersion (Sr1.5: 3.49, Sr2: 1.68, Sr3: 1.41, Sr5: 0.52 and Sr5,5: 1.23 % g mL^{-1}) was put in an Eppendorf tube. This tube is centrifuged at 2100 $\times g$ for two hours. Before characterization, the snowman particles in the tube were shaken and diluted to 0.5 % g mL^{-1}.

3.3.2 Functionalized particles

The functionalized Sr3 snowman particles were centrifuged at 2100 $\times g$ for one hour. This was sonicated for one hour and centrifuged at 2100 $\times g$ for one hour again. At each step a sample was withdrawn and observed with the optical microscope (OM).

3.4 Stability of snowman particles

The snowman particles are dispersed in aqueous solutions of varying pH and ionic strength to study their stability. Typical procedures were as follows: 1.5 µL 14 mM aqueous HCl solution, 13.5 µL 14 mM aqueous KCl solution and 140 µL water was added to an Eppendorf tube. After mixing, 45 µL Sr3 dispersion (1 % g mL^{-1}) was added. The final mixture was placed on a roller-table and was observed with the OM after one hour of rotation. The exact quantities and variations on the standard procedure are listed in table A.1.

3.5 Aggregation behavior of snowman particles with large microspheres

Typical procedures were as follows: 1.5 µL 14 mM aqueous HCl solution, 13.5 µL 14 mM aqueous KCl solution and 138 µL water were added to an Eppendorf tube. After shaking by hand, 45 µL snowman dispersion 1 % g mL^{-1} was added. The tube was shaken again and 2 µL microsphere dispersion (0.5 % g mL^{-1}) was added. The final mixture was placed on a roller-table and was observed with the OM after one hour of rotation. The exact quantities and variations on the standard procedure are listed in table A.2 and A.3.

3.6 Aggregation behavior of snowman particles with polymers

Typical procedures were as follows: 20 µL particle dispersion (1 % g mL^{-1}) and 175 µL water were added to an Eppendorf tube. After shaking, 5 µL bPEI solution (10 % g mL^{-1}) was added. The final mixture was placed on a roller-table and was observed with the OM after one hour of rotation. The exact quantities and variations on the standard procedure of bPEI are listed in table A.4 (seed particles) and A.5 (snowman particles). For lPEI the procedure is similar, but 14 mM HCl was added to dissolve lPEI in water. The exact quantities and variations on the standard procedure of lPEI are listed in table A.6.

3.7 Characterization

Hydrodynamic diameters were measured using a Malvern Zetasizer Nano instrument. The measurements were taken in seven runs of 15 individual measurements at a scattering angle of 173° and data was analyzed using the cumulant method of the Zetasizer software. The zeta potential was determined by laser Doppler electrophoresis at 173° using the same instrument. Here the Smoluchowski model was used to analyze the data.

Transmission electron microscope (TEM) pictures were taken with a Philips Technai 10 electron microscope typically operating at 100 kV. The samples were prepared by drying a drop of diluted aqueous colloid dispersion on top of polymer-coated copper grids, this drying was done under illumination with a heat lamp.

Scanning electron microscope (SEM) pictures were taken with a Philips XL FEG 30 SEM. The sample was freeze dried in order to keep the particle structures intact. For freeze-drying sample, 1 µL dispersion was brought on a polymer coated copper grid. The grid was vitrified in liquid nitrogen and mounted on a cryo transfer unit which was brought under vacuum of about 10^{-4} Pa. Temperature was increased to −90 °C at 5 °C min^{-1} and kept constant for about six hours under vacuum to allow the water to sublimate. These dried samples were sputter coated with 6 nm platinum prior to imaging.

Optical microscope (OM) images were made with Nikon Ti-E and Ti-U inverted microscopes. The used microscopy cell was constructed as follows: all glass slides were cleaned with water, ethanol and Kimtech precision wipes before use (figure 3.2a). Two coverslip glasses (VWR, #0, 22 x 22 mm) were placed at a distance of approximately 15 mm from each other on a microscope slide (Menzel-Gläser)

and fixated using tape. Subsequently, a drop of dispersion was injected in between the coverslips. The sample cell was then closed by taping an additional coverslip (Menzel-Gläser, #1.5, 22 x 22 mm on top of the two immobilized coverslips (figure 3.2b). The sample was monitored through the coverslip side of the sample cell. Fluorescence microscopy was done in a similar way with this microscope.

(a) Open (b) Closed

Figure 3.2: The microscope cell of the optical microscope without (open) and with (closed) sample.

Chapter 4

Results and discussion

4.1 Particles synthesis

4.1.1 Synthesis of positively charged large microspheres

The positively charged large microspheres were made by stabilizer free dispersion co-polymerization of styrene with METMAC. This polymerization method allows us to make particles with diameters from several hundred nanometers to several tens of micrometers. The particles are stabilized by the positive charges which are introduced by the co-monomer METMAC. After the polymerization the reaction mixture was washed immediately, otherwise microspheres tend to aggregate gradually to form big chunks.

Two types of microspheres with different size were synthesized, both of them are polydisperse. Figure 4.1a and 4.1b respectively show an optical microscope image and the size distribution (which was obtained by analyzing more than thousand particles on optical microscope images) of large microspheres. The large microspheres had a broad size distribution with an average diameter of 3.6 µm. These particles had a zeta potential of 55.7 ± 8.2 mV.

Figure 4.1c and 4.1d respectively show an optical microscope image and the size distribution (which was obtained by analyzing more than 75 particles on optical microscope images) of smaller microspheres. These microspheres had a small size distribution with an average diameter of 2.2 µm. These particles had a zeta potential of 45 ± 4.6 mV.

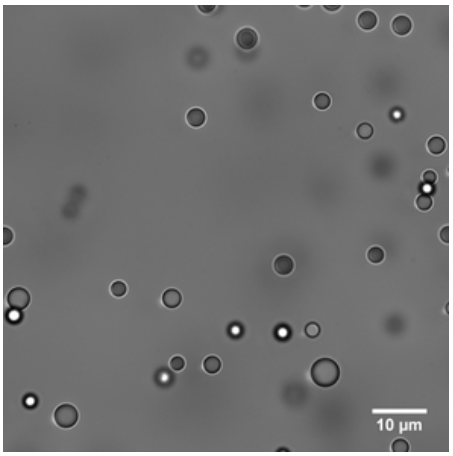

(a) Image of large microspheres

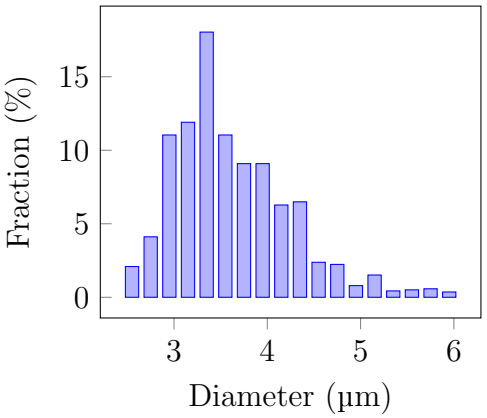

(b) Size distribution of large microspheres

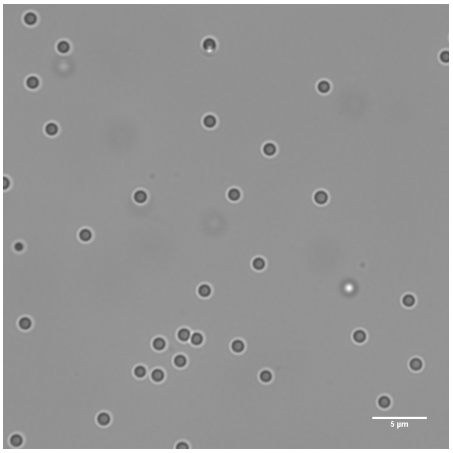

(c) Image of smaller microspheres

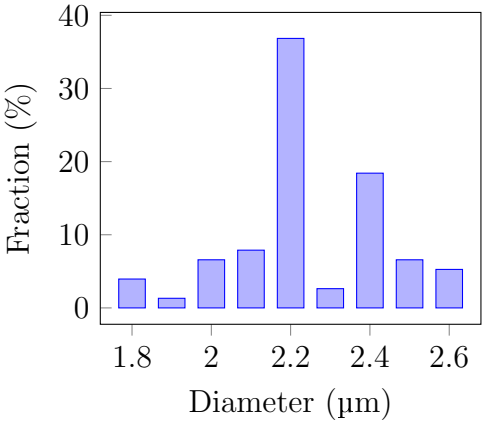

(d) Size distribution of smaller microspheres

Figure 4.1: Optical microscope image and size distribution of the large and smaller microspheres.

4.1.2 Synthesis of negatively charged snowman particles

Synthesis of seed particles

The negatively charged seed particles were made by emulsifier free emulsion co-polymerization of St with AA. This polymerization method allows us to make monodisperse particles with a size that is smaller compared to the microsphere, but big enough to be visible with an optical microscope. The particles are stabilized by the negative charges which are introduced by the initiator KPS and the co-monomer AA.

Figure 4.2a shows a TEM image of the seed particles. These particles are spherical and monodisperse with a size of 402 nm. Figure 4.2b shows a graph of the size and zeta potential (ζ) as a function of pH. With decreasing pH, the hydrodynamic diameter decreases from 455 nm to 425 nm and ζ increases from -53 mV to -33 mV. This decrease in size and increase in charge with decreasing pH is caused by the pH sensitive PAA-rich shell of the particle (section 2.2). However during the decrease of the hydrodynamic diameter between pH = 6 and 4, the zeta potential barely changes, which could be rationalized by counterion condensation. [24]

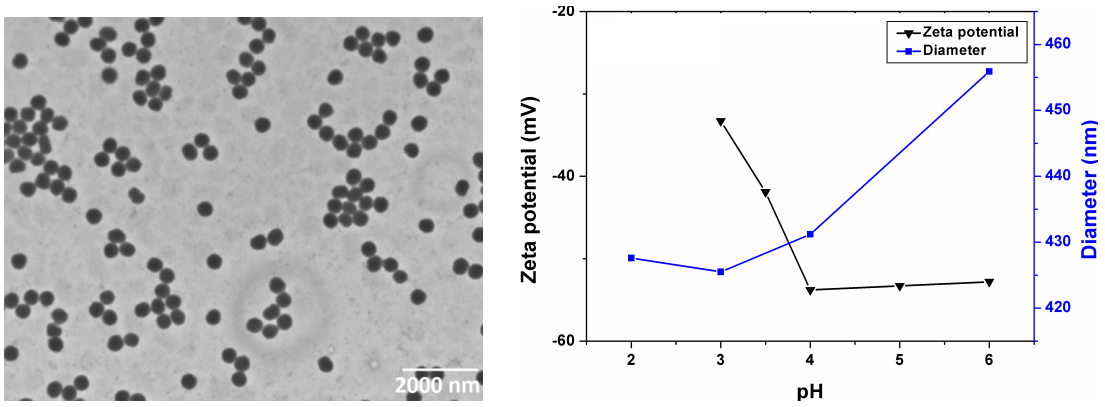

(a) TEM image

(b) Size and charge vs pH

Figure 4.2: A TEM image of the seed particles and a graph of the size and zeta potential of the seed particles as a function of pH.

Protrusion formation

A protrusion was grown on the seed particles and snowman particles with different head / body ratios were obtained (section 2.3 and 3.2.2). The protrusion is the "head" and the seed particle is the "body" of the snowman particle with the PAA-rich shell as "hairs" (figure 4.3).

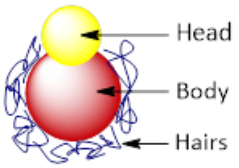

Figure 4.3: A scheme of the snowman particles with the head, body and hairs of the body indicated.

TEM images of these snowman particles were taken (figure 4.4). Sr1 has no head, Sr2 has a slightly smaller head than body, the head of Sr3 is slightly bigger than the body, Sr5 has a bigger head, Sr7 has very polydisperse particles and Sr9 has a big head with multiple small lobs on the body. Of these snowman particles only Sr2, Sr3 and Sr5 have suitable shapes for the mixing experiments. From these selected snowman particles the sizes were determined (table 4.1).

Table 4.1: The sizes and head / body ratio of the selected snowman particles.

Snowman type	Body radius (nm)	Head radius (nm)	Head / body volume ratio	Total length (nm)
Sr2	212	208	0.8	482
Sr3	230	244	1.3	671
Sr5	209	245	1.8	709

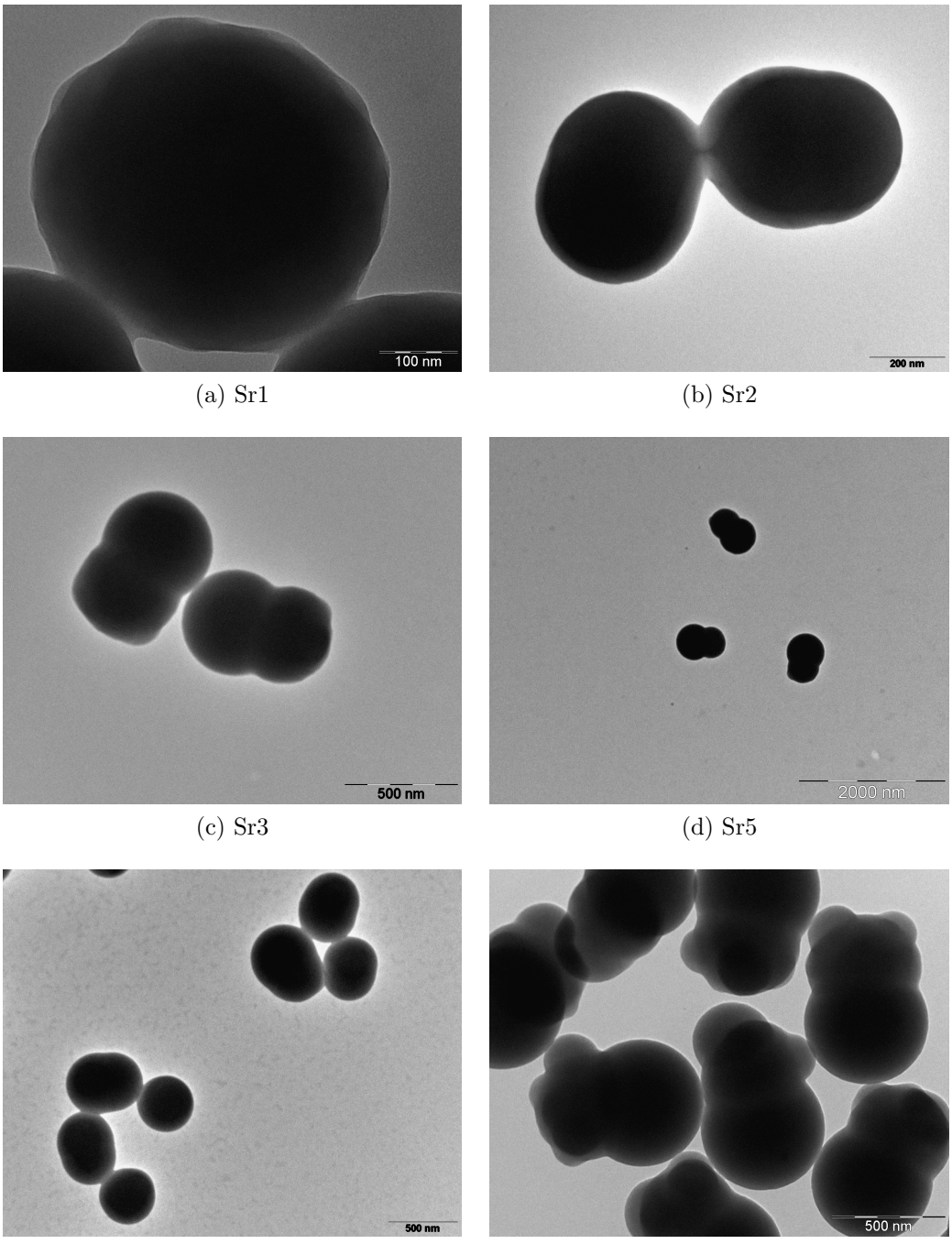

(a) Sr1 (b) Sr2

(c) Sr3 (d) Sr5

(e) Sr7 (f) Sr9

Figure 4.4: TEM images of the synthesized snowman particles with different swelling ratios.

4.2 Capsule formation test

According to Evers et al. snowman particles form hollow virus-like shells after centrifugation, especially if these particles are functionalized with FIA. In order to test if the snowman particles synthesized in section 4.1.2 also form these shells, non-functionalized and functionalized (with FIA) snowman dispersions are centrifuged (section 3.3).

In contrast to the snowman particles of Evers et al., none of these snowman dispersion formed shells. The non-functionalized snowman particles formed random aggregates instead of shells (figure 4.5a). Sr1.5 and Sr5.5 formed a few small aggregates, Sr2 and Sr3 formed some more small aggregates and Sr5 formed more aggregates that looked like rings or partial shells.
After the Sr3 dispersion was functionalized with FIA, it barely contained free particles and a lot of small and quite some big aggregates were present. This decrease in stability indicates that the snowman particles were functionalized. This succesfull functionalization was also confirmed with an fluorescence microscope. There was quite some background fluorescence, but the snowman particles were recognizable bright green, aldough it was hard to recognize if only the body or the whole particle is functionalized with FIA. The amount of aggregates were reduced after sonication, but after centrifugation still no shells were formed (figure 4.5b).

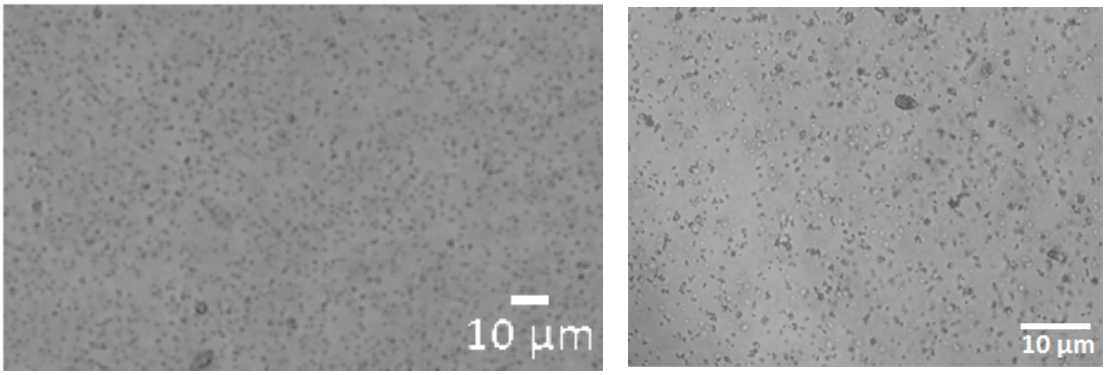

(a) Non-functionalized (b) Functionalized with FIA

Figure 4.5: Optical microscope images of the centrifuging experiments with Sr3 snowman particles with and without functionalization with FIA.

This abcence of shells could be caused by different surface properties. In contrast to Evers et al., no inhibitor was added during the polymerization of the protrusion. The absence of the inhibitor could have increased the hydrophobicity of the particles by causing additional crosslinked bumps on the surface of the particles. This

increase in hydrophobicity could have increased attraction between the particles too much. If the attraction is too strong, there is no reorientation to form ordered structures and only random aggregates are formed.

This increase in hydrophobicity could also explain the aggregates after the functionalization with FIA. The particles probably became too hydrophobic to be stable, since the functionalization with FIA makes the particles even more hydrophobic. Even when the snowman particles do not form shells upon centrifugation, it is still interesting to study the heteroaggregation of the particles with the microspheres.

4.3 Stability of snowman particles

Before studying the heteroaggregation behavior of snowman particles with large microspheres, the stability of Sr3 particles at different ionic strengths and pH values was investigated. At pH = 3 the particles at I = 1.0 mM and 10 mM were unstable, but at pH = 4 and 6 the particles at I = 1.0 mM and 10 mM were stable (figure 4.6). At pH = 3 the charge is too small, because pH is lower than the p*K*a of AA, hence the carboxyl acid groups are protonated (section 2.4.3). At pH = 4 the pH is also below the p*K*a, but it is close enough to have sufficient charge to stabilize the snowman particles. At pH = 6 the pH is above the p*K*a and the particle has a lot of charge which stabilizes the particles.

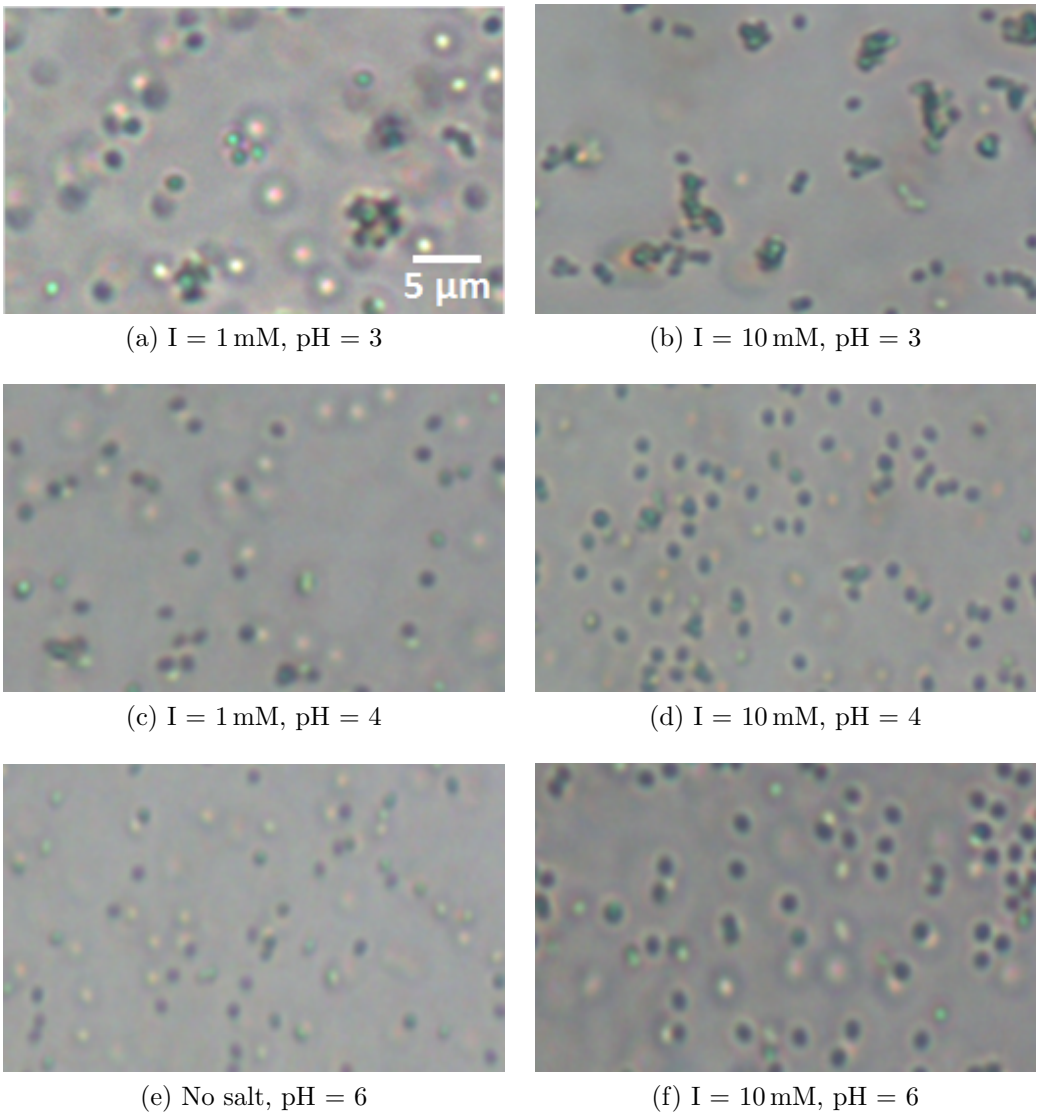

(a) I = 1 mM, pH = 3

(b) I = 10 mM, pH = 3

(c) I = 1 mM, pH = 4

(d) I = 10 mM, pH = 4

(e) No salt, pH = 6

(f) I = 10 mM, pH = 6

Figure 4.6: Sr3 particles at different ionic strengths and pH values.

4.4 Aggregation behavior of snowman particles with large microspheres

Large microspheres are mixed with snowman particles at different pH, I and roller-table times (t_{roll}) in order to study the influence of different conditions on the heteroaggregation (section 3.5). At each condition the coverage of microspheres by snowman particles is determined in terms of packing fractions. The amount of particles in a ring around the microsphere is divided by the maximum amount of particles at this ring to obtain this packing fraction. More information about the coverage and the orientation of the snowman particles is obtained from SEM images.

4.4.1 Influence of mixing time

To study when the aggregation is in equilibrium, the snowman particles were mixed with large microspheres at different t_{roll}. The snowman particles used were Sr1.5 and Sr3 (figure 4.7). The equilibrium coverage of Sr1.5 was reached after 50 minutes and Sr3 was in equilibrium after 60 minutes. With a short t_{roll} the coverage is lower than with a long t_{roll}, since the equilibrium coverage is not reached yet. After one hour all the samples have reached the equilibrium coverage so this t_{roll} is suitable to be used in further experiments.

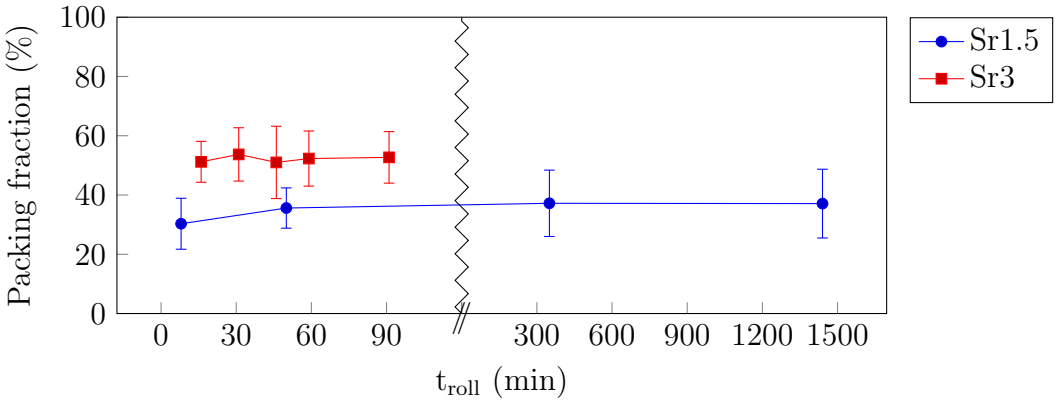

Figure 4.7: The influence of roller-table time (t_{roll}) on the coverage of the microspheres of Sr1.5 (blue circles) and Sr3 (red squares) in water. The standard deviation in packing fraction is indicated with error bars.

4.4.2 Influence of head size

The different snowman particles were mixed with the microspheres in water without salt or acid (figure 4.8 and 4.9). This was done to study the influence of the head size on the coverage and to get an indication of the coverage for them. Sr2 with the smallest head barely covered the microsphere, Sr5 with the biggest head covered the microsphere a little and Sr3 with a slightly bigger head than body almost completely covered the microsphere. All these snowman particles where stable, even Sr5 with an big head size. This stability indicates that some charge on the head is present.

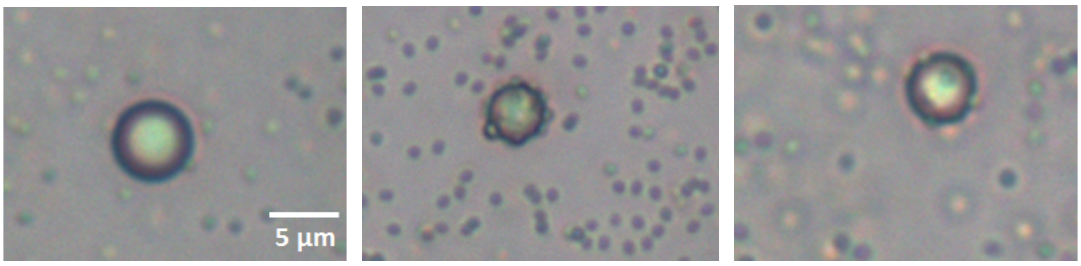

(a) Sr2 (b) Sr3 (c) Sr5

Figure 4.8: Optical microscope images of snowman particles on microspheres in water.

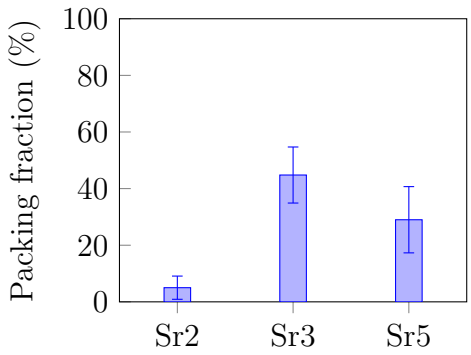

Figure 4.9: The coverage of the different snowman dispersion in water.

The low coverage of Sr2 is consistent with the coverage of the seed particle. This seems to indicate that the small head is not attractive enough to compensate for a certain repulsion force of the seed. With a big head (Sr5) the coverage is higher, but most of the microsphere is still not covered. An explanation for this could be that the big head is attractive enough to compensate a part of the repulsion force that was present in the seed.

The high coverage is obtained for the particles with the equally sized head (Sr3) is not in line with the coverages of the particles with a small and big head. With Sr3 a certain repulsion force seems to be absent, eventhough the surface functionalities are the same. The space between two Sr3 particles is too big for lateral repulsion since the Debye length (κ^{-1}) is in the order of 100 nm (equation B.1), but it could be caused by random sequential adsorption with repulsion.

The repulsion force that limits the coverage of Sr2 and Sr5 is already present in the seed particles. Yong et al. [25] propose that this is caused by leached PAA polymers of the seed particles. These PAA-rich polyelectrolytes leached from the particles into the continuous phase. When these negatively charged polymers adsorb on the microspheres, the charges of the microspheres are inversed and the snowman particles are repelled (figure 4.10). This could also explain the charge on the head, some of the leached polymers were incorporated when the protrusion was polymerized. If this is the case, the coverage should increase when the leached polymers are washed away. After washing, the coverage of Sr2 and Sr5 both were increased a lot and Sr3 increased a little (figure 4.11). The coverage seems to increase slightly with the head size of the particles, however this is hard to determine since the difference is smaller than the standard deviation. This increase in coverage after washing indicates that the leached polymers caused the repulsion of the snowman particles. Since the coverage of Sr3 is similar before and after washing, the high coverage before washing could be caused by a better washing step after Sr3 was synthesized.

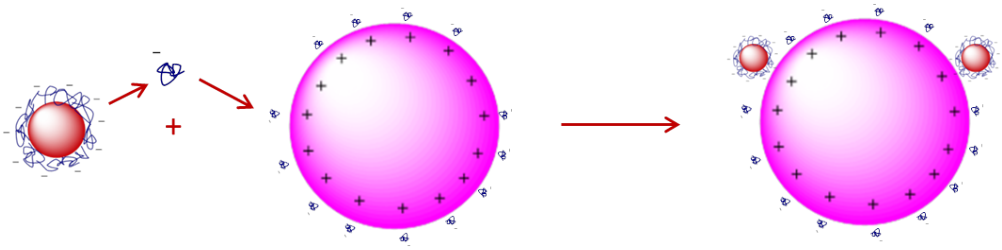

Figure 4.10: Schematic illustration of PAA leaching from the seed particles and adsorbing on a microsphere.

Unfortunately this cause of the low coverage was found at the end of the project, so the other experiments are done with unwashed particles. With these unwashed particles we study effects of the interplay between the PAA polymers and snowman particles by comparing the coverage of the microspheres under varying conditions.

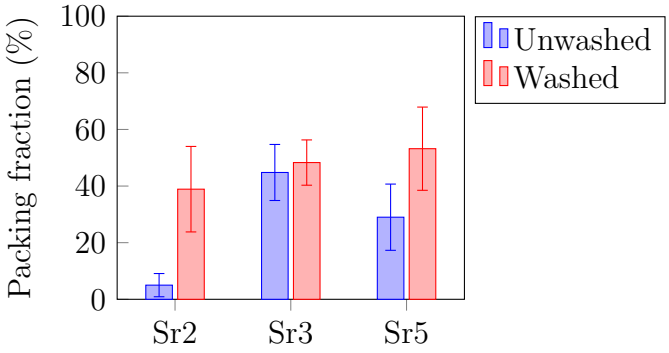

Figure 4.11: The coverage of the different snowman dispersion in water before (red) and after (blue) washing. The standard deviation in packing fraction is indicated with error bars.

4.4.3 Influence of ionic strength

The snowman dispersions were mixed with the microspheres in salt solutions with different concentrations at pH = 4 and 6 (figure 4.12 and 4.13). This was done to study the influence of the ionic strength (I) on the coverage of the microspheres. The coverage increased of all snowman particles when I was increased, especially Sr2 at pH = 6 between no salt and I = 1.0 mM. Sr2 and Sr5 had similar coverage except without salt. Sr3 had the highest coverage, the particles seem to touch each other instead of having a distance of approximately a particle between them.

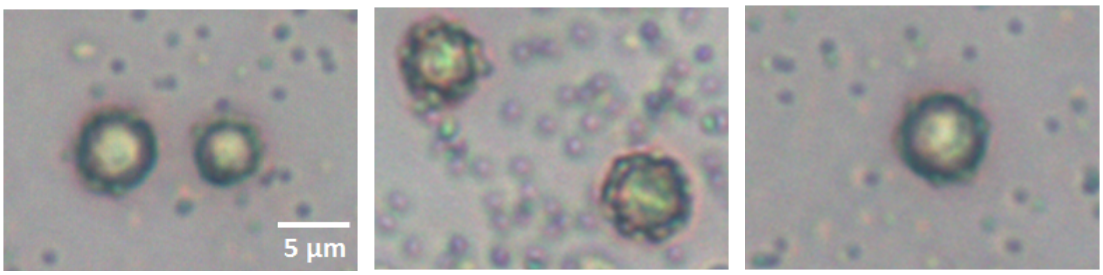

(a) Sr2 (b) Sr3 (c) Sr5

Figure 4.12: Optical microscope images of snowman particles on microspheres at pH = 6 and I = 20 mM.

When salt is added, the ionic strength increases and the effect of the electronic interactions decreases. With 20 mM salt the Debye length decreases to 2 nm (equation B.2). This means that the attraction between the microsphere and PAA (leached and of the snowman particles) decreases and the repulsion between the

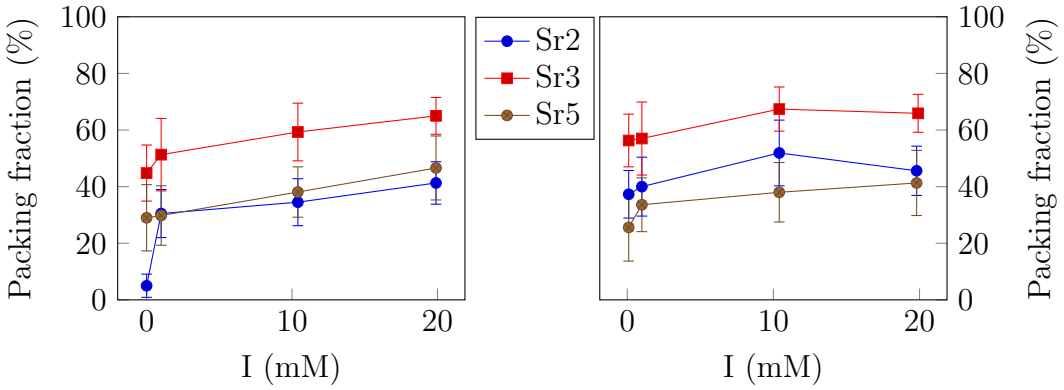

(a) pH = 6 (b) pH = 4

Figure 4.13: The influence of ionic strength (I) on the coverage of the microspheres of Sr2 (blue circles), Sr3 (red squares) and Sr5 (brown circles). The standard deviation in packing fraction is indicated with error bars.

snowman particles (and the leached PAA) decreases. However the hydrophobic attractive force of the head of the snowman particle is still the same. An explanation of the sudden increase in coverage of Sr2 could be that the repulsion is now small enough to be partially compensated by the attractive head. The increase in coverage of Sr2 and Sr5 with an increase in ionic strength is caused by the reduction of the electrostatic repulsion (between leached PAA and snowman particles) while the hydrophobic attraction stays constant. The increase in coverage of Sr3 is caused by the random sequential adsorption with less repulsion between the snowman particles.

4.4.4 Influence of pH

The snowman dispersions were mixed with the microspheres in solutions with different pH values at I = 1.0 mM and 10 mM (figure 4.14 and 4.15). This was done to observe a difference between the snowman particles in the influence of the pH on the coverage of the microspheres. The coverage of all snowman particles increased when the pH was decreased, especially below pH = 4 where the snowman started to be unstable. Between pH = 4 and 6, Sr2 had the biggest change, Sr3 had slightly less change and Sr5 barely had a change in the coverage.

When the pH is decreased, the charge of the snowman particle decreases and the hydrophobicity increases (section 2.4.3). For all snowman particles the coverage slowly increases with the decrease of pH, which is similar to the addition of salt

to the dispersion (section 4.4.3). Not only the charge of the snowman particles is reduced, but also the charge of the leached PAA is reduced, which results in less electrostatic repulsion. This decrease in repulsion combined with the increased hydrophobicity leads to a higher coverage. However when the repulsion is reduced too much, the snowman particles are unstable (section 4.3). At low pH values very high coverages are obtained, however aggregates of snowman particles are also formed.

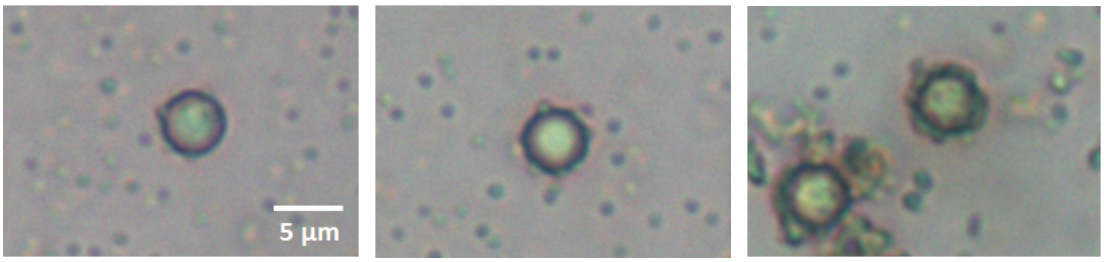

(a) pH = 6 (b) pH = 4 (c) pH = 3

Figure 4.14: Optical microscope images Sr2 on microspheres at I = 1 mM at different pH values.

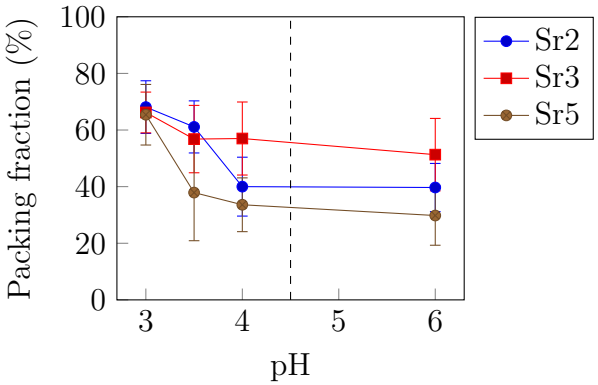

Figure 4.15: The influence of pH on the coverage at I = 1 mM of the microspheres of Sr2 (blue circles), Sr3 (red squares) and Sr5 (brown circles). The dashed line indicates the p*K*a value of AA. The standard deviation in packing fraction is indicated with error bars.

4.4.5 Influence of microsphere size

In the experiments above the amounts of particles on the microspheres and the size of these microspheres size were determined in order to calculate packing fraction. An average was taken over all particles for each sample to get the packing fraction of each sample. Here was assumed that the snowman particles have no preferred microsphere size. This assumption was made because there was no outstanding microsphere size during the first few experimients. To verify if this assumption is correct and no preferred microsphere size is present, the coverage of microspheres with different sizes was compared. For each sample, the coverage at different microsphere diameters seems similar (figure 4.17).

To study if at smaller microsphere sizes the affinity changes, the smaller microspheres are mixed with Sr2 and Sr3 at pH = 6 and I = 10 mM. For both samples, the coverage seems to be slightly decreasing with increasing diameter (figure 4.16). This indicates that the microsphere size barely has an effect on the packing fraction. This means that the assumption that there is no preferred microsphere size is feasible.

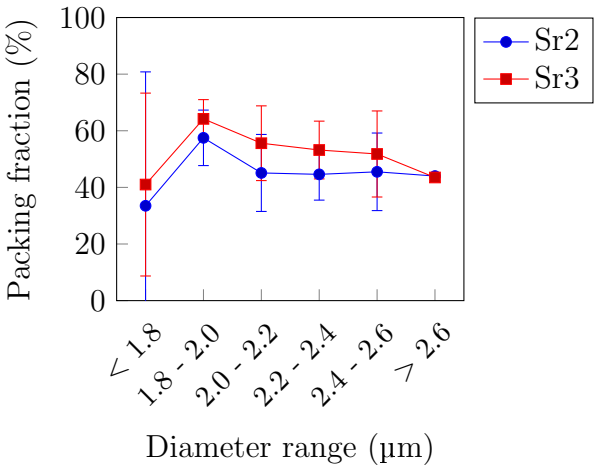

Figure 4.16: Influence of diameter on coverage of Sr2 (blue circles) and Sr3 (red squares) at pH = 6 with I = 10 mM. The standard deviation is indicated with error bars.

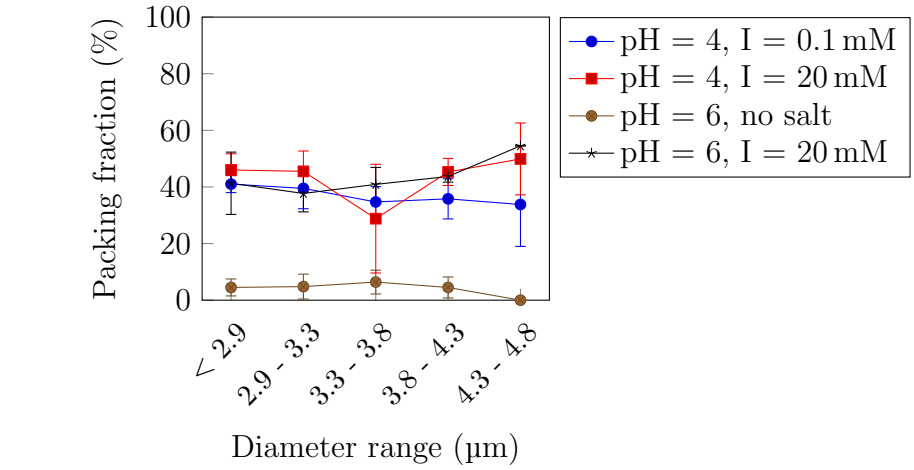

(a) Sr2

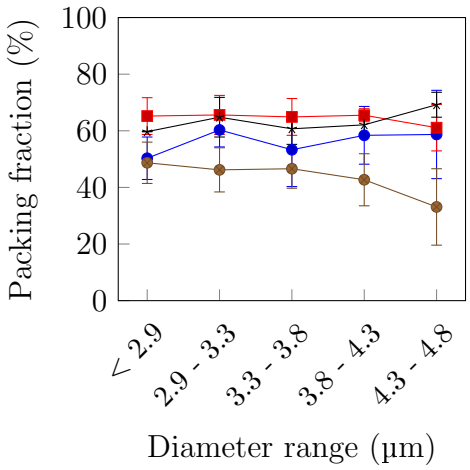

(b) Sr3

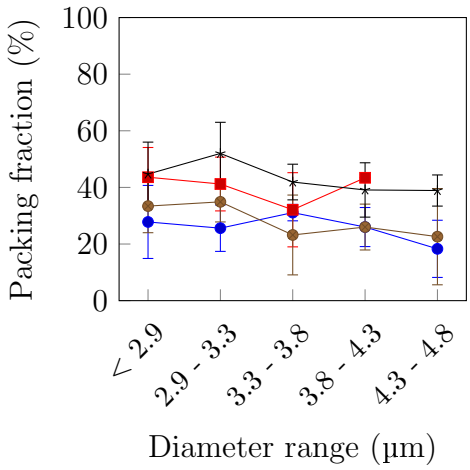

(c) Sr5

Figure 4.17: Influence of diameter on coverage of Sr2, Sr3 en Sr5 at pH = 4 with I = 0.1 mM (blue circles) and 20 mM (red squares) and at pH = 6 with no salt (brown circles) and 20 mM (black stars). The standard deviation is indicated with error bars.

4.4.6 Closer look at coverage and orientation

SEM pictures were taken of the freeze dried samples to observe the coverage in more detail and to study if there is a preferred orientation of the snowman particles. The freeze dried samples consists of microspheres mixed with Sr3 (pH = 4, I = 10 mM) and Sr5 (pH = 3.5, I = 1 mM).

Coverage

With the optical microscope, 57 and 38 % coverage are observed for the Sr3 and Sr5 samples respectively (section 4.4.3 and 4.4.4). Here the particles seem to touch each other, which could indicate a close packed structure. However the SEM images indicate that the particles are adsorbed in an open structure (figure 4.18). This means that the particles do not form a closely packed shell. This indicates the method to determine the packing fraction (by optical microscopy) is not acurate enough to determine the actual packing fraction. The amount of particles in a ring was counted and then divided by the maximum coverage of spheres. Due to the low resolution the microsphere size could have been approximated wrong. This low resolultion also causes the snowman particles to appear as spheres on the image even though they consist of two lobs. Because they appear as a sphere, all snowman particles where approximated as a sphere of a certain size. However this could have caused a small error in the approximation of the coverage between the different snowman sizes.
It is possible that too many particles were counted, because some particles could be double counted or wrongly counted. Some particles that were just above or just below the circle could have been wrongly counted, since they were also in focus. Snowman particles could also have been double counted if they appeared as two adjacent spheres.

Orientation

The orientation of the snowman particles on the microsphere differs for the two samples with high coverage (figure 4.18), here the rough lob is the body and the smooth lob is the head. The snowman particle can be attached with both the head and body (parallel) or it can be attached with one of them. The snowman can be attached with an angle or perpendicular to the microsphere. For Sr3 the number of parallel and perpendicular snowman particles are almost the same and around a fifth of the particles has angle. There seems no preference for the head or the body to be attached to the microsphere, however there are patches with

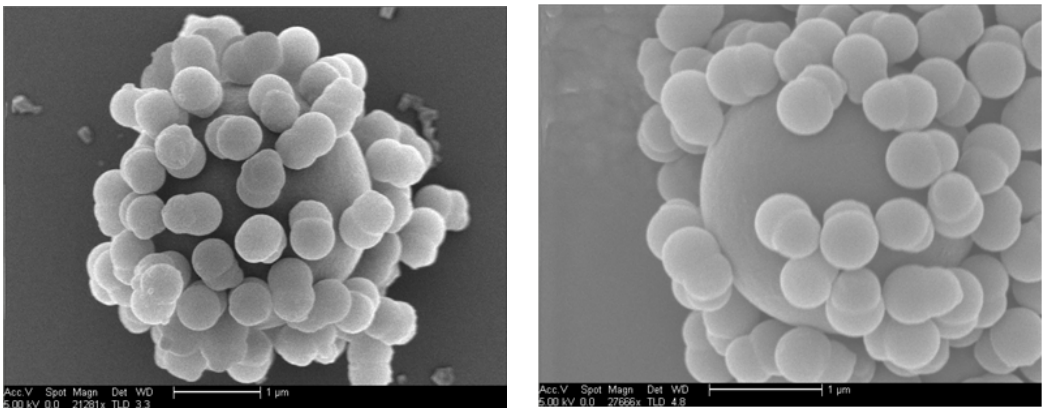

(a) Sr3 at pH = 4, I = 10 mM (b) Sr5 at pH = 3.5, I = 0.3 mM

Figure 4.18: SEM pictures of snowman particles on the microspheres.

particles that have similar orientations. For Sr5 most of the snowman particles are parallel with both lobs on the microsphere. The number of perpendicular particles and those with an angle are both around a fifth of the particles, here seems to be a slight preference for the body to be attached to the microsphere. Also under this condition patches with particles that have similar orientations are present. However it is hard to say if the difference in orientation is due to the particle type or due to the increased pH or ionic strength of the dispersion.

4.5 Aggregation behavior of snowman particles with polymers

To study the influence of the polymers on the heteroaggregation, the snowman particles and seed particles are mixed with PEI (section 3.6). This is done with different amounts of bPEI and seed particles, to investigate the effect of the particle and polymer concentrations. Also snowman particles were mixed different amounts of bPEI, in order to determine if more stability is obtained when the head size is increased. The effect of the density of the polymer is also studied by mixing lPEI with Sr3 at pH = 4.

4.5.1 Phase diagram of seed particles

Before we study the effect of the head size on the heteroaggregation behavior of snowman particles, we need to know the stability of the seed particles. Different concentrations of seed particles are mixed with different amounts of bPEI (figure 4.19 and 4.20). At a $\varphi_p = 1 \times 10^{-7}\,\mathrm{mL/mL}$ all the seed particles are still stable. At $\varphi_p = 2.5 \times 10^{-7}\,\mathrm{mL/mL}$ some small clusters were formed for each sample. More PEI is needed to reach the point where the seed particles switch from some small clusters to big clusters when the seed concentration is increased. The shift of this point is due to the different polymer/particle number ratios. At low seed concentration there are more polymers per seed particle than at high seed concentrations. However when the number ratio is too high, the sample becomes stable again. This is probably caused by the inversion of the charge, which causes the particles to repel each other again.

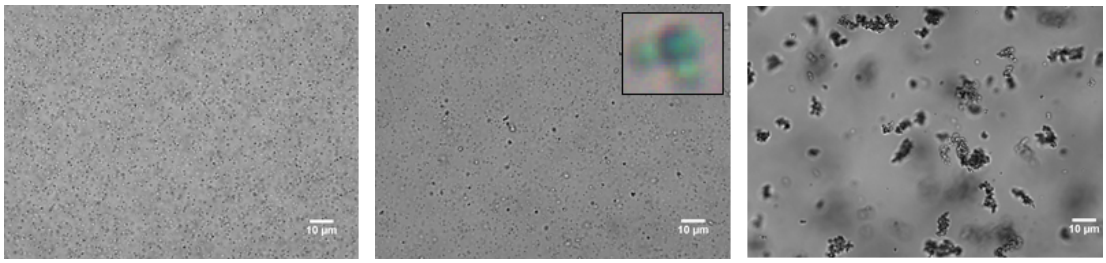

(a) No clusters (b) Small clusters (c) Big clusters

Figure 4.19: Optical microscope images of different stability regions of the seed particles, the inset shows an example of a "small cluster". With $\varphi_{seed} = 6.7 \times 10^{-4}\,\mathrm{mL/mL}$ and a) $\varphi_p = 1.0 \times 10^{-7}\,\mathrm{mL/mL}$, b) $\varphi_p = 5.0 \times 10^{-7}\,\mathrm{mL/mL}$, c) $\varphi_p = 8.8 \times 10^{-6}\,\mathrm{mL/mL}$.

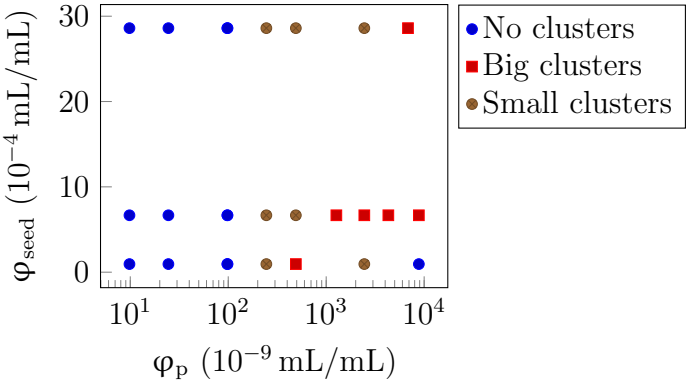

Figure 4.20: The influence of φ_p at different φ_{seed} on the stability. The stability regions are: no clusters (blue circles), small clusters (brown circles) and big clusters (red squares).

4.5.2 The influence of head size

To study if the head of the snowman particles sterically stabilize the aggregation, snowman particles with different head sizes were mixed with bPEI (figure 4.21). The amounts of small and big clusters at two interesting regions are also determined. One of this regions is at number ratio = 1000 for Sr2, 3, and 5 (figure 4.22a). The other region is of Sr5 for number ratios 500, 1000 and 2000 (figure 4.22b). At a number ratio of 100 ($\varphi_p \approx 1.0 \times 10^{-7}$ mL/mL) all the particles are still stable. After a number ratio of 1000 ($\varphi_p \approx 1.0 \times 10^{-6}$ mL/mL) almost all the particles are completely unstable. Only at a swelling ratio of 5 the particles are a bit unstable. A higher polymer concentration is needed for the particles to become completely unstable. This happens at a number ratio of 2500 ($\varphi_p = 1.1 \times 10^{-6}$ mL/mL). This means that swelling ratios of 3 and lower (slightly smaller and slightly bigger head) is not enough to sterically stabilize the aggregation due to the polymer. At a swelling ratio of 5 (big head) a bit of sterical stabilization seems to be present, because more polymers are needed for complete instability.

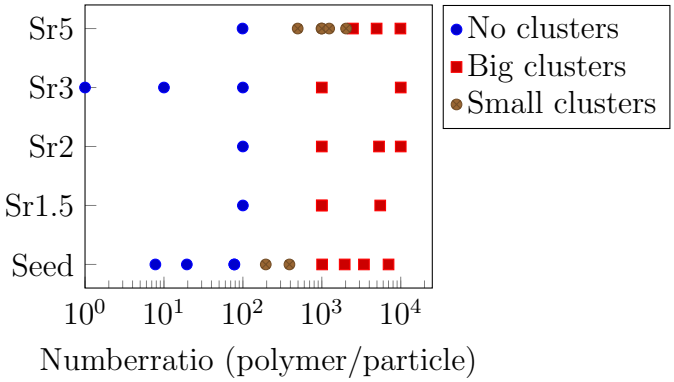

Figure 4.21: The influence of φ_p with different snowman particles on the stability. The stability regions are: no clusters (blue circles), small clusters (brown circles) and big clusters (red squares).

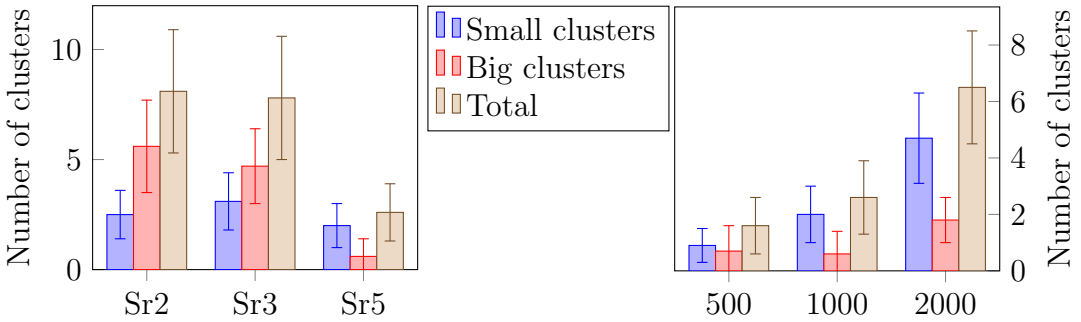

(a) Number ratio = 1000 (b) Sr5

Figure 4.22: The average number of small (blue), big (red) and the total amount of clusters (brown) in a 120x90 µm picture. The standard deviation is indicated with error bars.

4.5.3 The influence of polyelectrolyte type

To study the effect of the polyelectrolyte type, Sr3 was mixed at pH = 4 with lPEI. This polymer has around half of the weight, but the radius of gyration (Rg) is similar (section B.2). The stability at different concentrations of lPEI were observed (figure 4.23) and amount of small and big clusters was determined (figure 4.24). At the number ratio of 100 and 1000 ($\varphi_p = 1.5 \times 10^{-8}$ mL/mL and 1.5×10^{-7} mL/mL) Sr3 was a bit unstable and at the number ratio of 10000 ($\varphi_p = 1.5 \times 10^{-6}$ mL/mL) Sr3 was completely unstable. At low polymer concentrations, the samples with lPEI were less stable than the samples with bPEI. However the bPEI samples were at pH = 6 and the lPEI samples were at pH = 4, so this could also be an effect of the pH instead of the polyelectrolyte type.

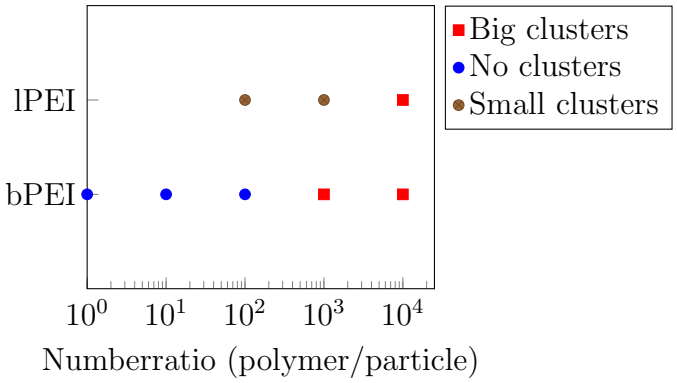

Figure 4.23: The influence of the polymer volume fraction (φ_p) with bPEI (pH = 6) and lPEI (pH = 4) on the stability of Sr3. The stability regions are: no clusters (blue circles), small clusters (brown circles) and big clusters (red squares).

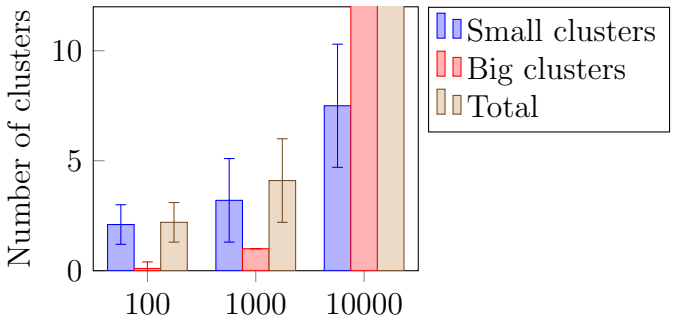

Figure 4.24: The average number of small (blue), big (red) and the total amount of clusters (brown) in a 120x90 µm picture. The standard deviation is indicated with error bars.

Chapter 5

Conclusion

Large positively charged large microspheres were made. The large microspheres had a zeta potential of $55.7 \pm 8.2\,\mathrm{mV}$, a broad size distribution and average diameter of $3.6\,\mu\mathrm{m}$. Also pH responsive negatively charged seed particles were made. When the pH is reduced from 6 to 3, the zeta potential increases from $-53\,\mathrm{mV}$ to $33\,\mathrm{mV}$ and the diameter decreases from $425\,\mathrm{nm}$ to $455\,\mathrm{nm}$. Three useful types snowman particles were made of these seed particles. The three types have different protrusion sizes: smaller, equal and bigger compared to the seed particle. The snowman particles are monodisperse and have protrusion/seed volume ratio of 0.8, 1.3 and 1.8 respectively. A part of the snowman particles with equally sized seed and protrusion was fluorescently labeled. However this caused the particles to become unstable. Both these particles and the non-functionalized snowman particles were centrifuged, but no virus-like shells were formed.

All non-functionalized snowman particles are stable at ionic strengths between $10^{-2}\,\mathrm{mM}$ (Millipore water) and $20\,\mathrm{mM}$ and at pH values between 4 and 6. Below pH = 4, the snowman particles are unstable and form aggregates. After an hour the aggregation of snowman particles on the microspheres is in equilibrium. The size of the microspheres has little influence on the coverage. The snowman particle with the smallest protrusion has a low coverage in pure water. This low coverage is consistent with the coverage of the seed particles. The snowman with the biggest protrusion has higher coverage, but the one with a medium protrusion has the highest coverage. The coverage was limited by leaching polymers of the particles, since the coverage increased after the snowman particles were washed. The coverage of the snowman types with the smallest and biggest protrusion increased a lot and the coverage of the snowman type with the medium protrusion increased slightly. This results in similar coverage for all snowman types, although there is a slight increase with increasing protrusion size. The coverage increases

for all unwashed snowman types when the ionic strength is increased and when the pH is decreased. Even with high coverages, the snowman particles do not form a close packed structure on the microspheres. Also no preferred orientation of the snowman particles was observed.

The seed particles and all unwashed snowman types aggregate, when sufficient oppositely charged polymers are added, At a number ratio of 1000 polymers/particles, the aggregation of the seed particles switches from small to big clusters. This transition point is similar for the snowman types with the small and medium protrusion, but it is shifted for the snowman type with the biggest protrusion. The shift of this point is to higher polymer concentrations, which indicates that sterical stabilization is present.

Chapter 6

Outlook

There are some interesting experiments to be done with the snowman particles. The seed particles reversibly attach to the microspheres when the pH is decreased and increased again due to the loose polymers. Since the snowman particles also have the loose polymers they could also reversibly attach, but this could also be inhibited by the protrusion. To have a better look on the effect of these polymers, the experiments with the unwashed and the washed particles can be compared. In order to do this, more experiments with the washed particles at different ionic strengths and pH values are needed. Other particles to do these experiments with are snowman particles that form shells upon centrifugation, since they might also form these shells around the microspheres. For these experiments, the coverage can be determined in number of particles per area instead of per ring, since the number of particles per ring is inaccurate. This coverage determination can also be done from SEM images which also give information about the orientation of the snowman particles. However each sample needs to be freeze-dried before it can be observed by SEM.

To see the effect of the protrusion better, a snowman type with a very large protrusion should be mixed with the microspheres and polymers. This could increase the coverage of the microspheres and decrease the formation of large random clusters. In order to see the small protrusion also decreases the formation of these large clusters, more experiments are needed with polymer concentrations around 1000 polymers per particle. Also more experiments are needed with seed particles and different snowman particles in order to see the effect of the linear polymer. In order to compare the linear and the branched polymer, the snowman particles should be mixed with the branched polymer at a pH of four. Different ionic strength, another polymer type and washed snowman particles would also be interesting to study.

Chapter 7

Acknowlgements

I would like to thank my daily supervisor Yong Guo for his support. He gave me some of his particles, he helped me to come up with the next steps for the experiments and he explained the things that I misunderstood or did not understand. I would also like to thank my other supervisor Willem Kegel for his useful discussions and interesting ideas. Also the rest of the FCC group especially the master room, I would like to thank for the mental support and the nice time I had during my thesis. Last but not least, I would like to thank my family for the mental support, food and love they gave me during my thesis and during the rest of my life.

Bibliography

[1] Chris H. J. Evers, Jurriaan A. Luiken, Peter G. Bolhuis, and Willem K. Kegel. Self-assembly of microcapsules via colloidal bond hybridization and anisotropy. *Nature*, 534(7607):364–368, 2016.

[2] Anetta Undas and Robert A S Ariëns. Fibrin clot structure and function: A role in the pathophysiology of arterial and venous thromboembolic diseases. *Arteriosclerosis, Thrombosis, and Vascular Biology*, 31(12), 2011.

[3] T Croguennec, F Nau, and G Brule. Influence of pH and salts on egg white gelation. *Journal of Food Science*, 67(2):608–614, 2002.

[4] Fabrizio Chiti and Christopher M. Dobson. Protein Misfolding, Functional Amyloid, and Human Disease. *Annual Review of Biochemistry*, 75(1):333–366, 2006.

[5] George M. Whitesides and Bartosz Grzybowski. Self-Assembly at All Scales. *Science*, 295(5564):2418–2421, 2002.

[6] George M Whitesides and Mila Boncheva. Beyond molecules: self-assembly of mesoscopic and macroscopic components. *Proceedings of the National Academy of Sciences of the United States of America*, 99(8):4769–74, 2002.

[7] Elizabeth J. Tanner, Karla A. Kirkegaard, and Leor S. Weinberger. Exploiting Genetic Interference for Antiviral Therapy. *PLoS Genetics*, 12(5):1–14, 2016.

[8] Colloid: Properties of Colloids. In *The Columbia Electronic Encyclopedia*. Columbia University Press, 6 edition, 2012.

[9] Mark S. Elliot and Wilson C. K. Poon. Conventional optical microscopy of colloidal suspensions. *Advances in Colloid and Interface Science*, 92(1-3):133–194, 2001.

[10] B. Vincent, C. Young, and T. Tadros. Equilibrium Aspects of Heteroflocculation in Mixed. *Faraday Discuss*, 65:296–305, 1978.

[11] Brian Vincent, Miguel Jafelicci, Paul F. Luckham, and Tharwat F. Tadros. Adsorption of small, positive particles onto large, negative particles in the presence of polymer. Part 2.—Adsorption Equilibrium and Kinetics as a Function of Temperature. *Journal of the Chemical Society, Faraday Transactions 1: Physical Chemistry in Condensed Phases*, 76:674–82, 1980.

[12] Stephen Harley, Dudley W. Thompson, and Brian Vincent. The adsorption of small particles onto larger particles of opposite charge Direct electron microscope studies. *Colloids and Surfaces*, 62(1-2):153–162, 1992.

[13] Philip Lijnzaad, Herman J. C. Berendsen, and Patrick Argos. Hydrophobic Patches on the Surfaces of Protein Structures. *PROTEINS: Structure, Function, and Genetics*, 25:389–397, 1996.

[14] Gérard Riess. Micellization of block copolymers. *Progress in Polymer Science (Oxford)*, 28(7):1107–1170, 2003.

[15] Yufeng Wang, Yufeng Wang, Dana R Breed, Vinothan N Manoharan, Lang Feng, Andrew D Hollingsworth, Marcus Weck, and David J Pine. Colloids with valence and specific directional bonding. *Nature*, 491(7422):51–5, 2012.

[16] Shan Jiang, Qian Chen, Mukta Tripathy, Erik Luijten, Kenneth S. Schweizer, and Steve Granick. Janus particle synthesis and assembly. *Advanced Materials*, 22(10):1060–1071, 2010.

[17] Emanuela Bianchi, Ronald Blaak, and Christos N. Likos. Patchy colloids: state of the art and perspectives. *Physical Chemistry Chemical Physics*, 13(14):6397–410, 2011.

[18] Qingquan Liu, Yanlu Li, Shaohua Shen, Zhihua Zhou, Boli Ou, and Shuanli Tang. Preparation of Monodisperse Cationic Microspheres by Dispersion Polymerization of Styrene and a Cation-Charged Monomer in the Absence of a Stabilizer. *Journal of Macromolecular Science, Part A: Pure and Applied Chemistry*, 48(7):518–525, 2011.

[19] P. H. Wang and C.-Y. Pan. Preparation of styrene/acrylic acid copolymer microspheres: Polymerization mechanism and carboxyl group distribution. *Colloid and Polymer Science*, 280(2):152–159, 2002.

[20] Xin Hu, Huarong Liu, Xueping Ge, Song Yang, and Xuewu Ge. Preparation of Submicron-sized Snowman-like Polystyrene Particles via Radiation-induced Seeded Emulsion Polymerization. *Chemistry Letters*, 38(8):854–855, 2009.

[21] Eric B. Mock, Hank De Bruyn, Brian S. Hawkett, Robert G. Gilbert, and Charles F. Zukoski. Synthesis of anisotropic particles by seeded emulsion polymerization. *Langmuir*, 22:4037–43, 2006.

[22] Istvan Szilagyi, Dana Rosicka, Jose Hierrezuelo, and Michal Borkovec. Charging and stability of anionic latex particles in the presence of linear poly(ethylene imine). *Journal of Colloid and Interface Science*, 360(2):580–585, 2011.

[23] Małgorzata Wisniewska, Teresa Urban, Elzbieta Grzadka, Vladimir I. Zarko, and Vladimir M. Gun'ko. Comparison of adsorption affinity of polyacrylic acid for surfaces of mixed silica-alumina. *Colloid and Polymer Science*, 292(3):699–705, 2014.

[24] D Stigter. Evaluation of the counterion condensation theory of polyelectrolytes. *Biophys journal*, 2(69):380–8, 1995.

[25] Yong Guo, Bas G. P. van Ravensteijn, Chris H.J. Evers, and Willem K. Kegel. Reversible encapsulation of micron-sized large colloids by oppositely charged submicron-sized small colloids. *To be published.*

[26] Chongbo Sun, Tian Tang, Hasan Uludag, and Javier E Cuervo. Molecular Dynamics Simulations of DNA / PEI Complexes : Effect of PEI Branching and Protonation State. *Biophysical Journal*, 100(June):2754–2763, 2011.

Appendix A

Variations on standard procedures

Table A.1: Variations of the standard procedure in the stability experiments.

HCl (µL)	KCl (µL)	Water (µL)
0	0	155.0
0	150.0	5.00
1.50	13.50	140.0
1.50	148.5	5.00
15.00	0	140.0
15.00	135.0	5.00

Table A.2: Roller-table time (t_{roll})variations on the standard procedure in the microsphere mixing experiments.

Snowman type	HCl (µL)	KCl (µL)	Water (µL)	t_{roll} (min)
Sr1.5*	150.0	0	0	5, 25, 45
Sr1.5*	135.0	15.00	0	8, 50, 350, 1440
Sr3	150.0	0	3.00	15, 30, 45, 60, 90

* 5 µL microspheres instead of 2 µL.

Table A.3: Other variations on the standard procedure in the microsphere mixing experiments.

Snowman type	14 mM HCl (µL)	14 mM KCl (µL)	28 mM KCl (µL)	Water (µL)
Sr2, Sr3, Sr5	0	0	0	153.0
Sr2, Sr3, Sr5	0	1.00	0	138.0
Sr2	0	72.0	0	81.0
Sr3	0	118.0	0	35.0
Sr2, Sr3, Sr5	0	150.0	0	3.00
Sr3	0	0	107.0	46.0
Sr2, Sr3, Sr5	0	0	142.0	11.00
Sr2, Sr3, Sr5	1.50	0	0	151.5
Sr2, Sr3, Sr5	1.50	13.50	0	138.0
Sr2	1.50	70.5	0	81.0
Sr3	1.50	116.5	0	35.0
Sr2, Sr3, Sr5	1.50	148.5	0	3.00
Sr3	1.50	0	106.2	46.8
Sr2, Sr5	1.50	0	140.8	10.70
Sr3	1.50	0	141.2	11.00
Sr2, Sr3, Sr5	4.50	10.50	0	138.0
Sr3	4.50	145.5	0	3.00
Sr2, Sr3, Sr5	15.00	0	0	138.0
Sr2, Sr3, Sr5	15.00	135.0	0	3.00
Sr3	45.0	105.0	0	3.00

Table A.4: The exact quantities of the variations in added bPEI to the seed particles. All these variations are with 2 µL, 20 µL and 60 µL seed dispersion.

Concentration (10^{-6} g mL^{-1})	Added (µL)
1.01	2.00
1.01	5.00
1.01	20.00
101	2.00
101	5.00
101	10.00
101	50.0
101	140.0
101	180.0

Table A.5: The exact quantities and variations on the standard procedure of bPEI with snowman particles.

Snowman type	bPEI solution Concentration (10^{-6} g mL^{-1})	Added (µL)	Water (µL)
Sr3	1.01e-3	8.80	17.2
Sr3	1.01e-3	88.0	92.0
Sr3	1.01e-2	88.0	92.0
Sr3, Sr5	1.01	8.80	171.2
Sr1.5	1.01	16.00	164.0
Sr2	1.01	16.60	163.4
Seed	1.01	25.7	154.3
Sr3, Sr5	1.01	44.0	136.0
Sr3	1.01	66.0	158.0
Seed, Sr1.5, Sr2, Sr3, Sr5	1.01	88.0	92.0
Sr5	1.01	89.0	91.0
Sr5	1.01	110.0	70.0
Sr1.5	1.01	160.0	20.00
Sr2	1.01	166.0	14.00
Sr5	1.01	180.0	0
Sr5	101	1.10	178.9
Sr1.5	101	1.60	178.4
Seed	1.01	257.0	0
Seed*	1.01	185.4	0

Continued on next page

Table A.5 – Continued

Snowman type	bPEI solution Concentration (10^{-6} g mL^{-1})	Added (µL)	Water (µL)
Seed*	10.1	18.50	166.9
Seed*	101	1.90	183.5
Sr5	101	2.20	177.8
Seed	101	2.60	177.4
Sr5	101	4.40	175.6
Seed, Sr1.5, Sr2, Sr3, Sr5	101	8.80	171.2
Sr2	101	16.60	163.4

* 14.60 µL snowman dispersion instead of 20.00 µL.

Table A.6: The exact quantities and variations on the standard procedure of lPEI.

bPEI solution Concentration (10^{-6} g mL^{-1})	Added (µL)	14 mM HCl (µL)	Water (µL)
50.0	7.10	1.30	191.6
1.00	35.6	1.40	163.0
1.00	3.60	1.40	195.0

Appendix B

Calculations

B.1 Debye length

The Debye length (κ^{-1}, equation 2.2) was calculated in order to determine at which distance the particles repel each other. This is done for water with (20×10^{-3} M) and without salt (10^{-5} M) at 25 °C. The Debye length without salt is 96 nm (equation B.1) and the Debye length with 20 mM salt is 2 nm (see equation B.2).

$$\kappa^{-1}(\mathrm{nm}) = \frac{3.04}{\sqrt{I(\mathrm{M})}} = \frac{3.04}{\sqrt{10^{-5}}} = 96\,\mathrm{nm} \tag{B.1}$$

$$\kappa^{-1}(\mathrm{nm}) = \frac{3.04}{\sqrt{I(\mathrm{M})}} = \frac{3.04}{\sqrt{20 \times 10^{-5}}} = 2.1\,\mathrm{nm} \tag{B.2}$$

B.2 Radius of gyration

The radius of gyration (Rg) is calculated for both the lPEI and bPEI. The amount of segments of the used polymer is for the bPEI 580 (equation B.3) and for lPEI 230 (equation B.4).

$$n_{\mathrm{br}} = \frac{M_{\mathrm{br}}}{m_{\mathrm{PEI}}} = \frac{25\,000\,\mathrm{g\,mol^{-1}}}{43.04\,\mathrm{g\,mol^{-1}}} \approx 580 \tag{B.3}$$

$$n_{\mathrm{li}} = \frac{M_{\mathrm{li}}}{m_{\mathrm{PEI}}} = \frac{10\,000\,\mathrm{g\,mol^{-1}}}{43.04\,\mathrm{g\,mol^{-1}}} \approx 230 \tag{B.4}$$

The length of these segments depends on the material. For a polymer with 13 segments the Rg of branched PEI is 6.5 Å and for linear PEI 9 Å. [26] Here the length of a branched segment is 1.8 Å (θ solvent, 1.4 Å for good solvent, equation B.5) and the length of a linear segment is 1.9 Å (θ solvent, 2.5 Å for good solvent, equation B.6).

$$\begin{aligned} \theta\ solvent : l_{\mathrm{br}} &= \frac{Rg_{\mathrm{br}}}{\sqrt{n_{\mathrm{br}}}} = \frac{6.5\,\text{Å}}{\sqrt{13}} = 1.4\,\text{Å} \\ good\ solvent : l_{\mathrm{br}} &= \frac{Rg_{\mathrm{br}}}{(n_{\mathrm{br}})^{3/5}} = \frac{6.5\,\text{Å}}{(13)^{3/5}} = 1.8\,\text{Å} \end{aligned} \tag{B.5}$$

$$\begin{aligned} \theta\ solvent : l_{\mathrm{li}} &= \frac{Rg_{\mathrm{li}}}{\sqrt{n_{\mathrm{li}}}} = \frac{9\,\text{Å}}{\sqrt{13}} = 1.9\,\text{Å} \\ good\ solvent : l_{\mathrm{li}} &= \frac{Rg_{\mathrm{li}}}{(n_{\mathrm{li}})^{3/5}} = \frac{9\,\text{Å}}{(13)^{3/5}} = 2.5\,\text{Å} \end{aligned} \tag{B.6}$$

Now the length of the segments and the amount of segments are known, so we can calculate the Rg of both polymers. The Rg of the bPEI is 43 Å (θ solvent, 63 Å for good solvent equation B.7) and of the lPEI it is 38 Å (θ solvent, 50 Å for good solvent equation B.8).

$$\begin{aligned} \theta\ solvent : Rg_{\mathrm{br}} &= \sqrt{n_{\mathrm{br}}} \cdot l_{\mathrm{br}} = \sqrt{580} \cdot 1.8\,\text{Å} = 43\,\text{Å} \\ good\ solvent : Rg_{\mathrm{br}} &= (n_{\mathrm{br}})^{3/5} \cdot l_{\mathrm{br}} = (580)^{3/5} \cdot 1.4\,\text{Å} = 63\,\text{Å} \end{aligned} \tag{B.7}$$

$$\begin{aligned} \theta\ solvent : Rg_{\mathrm{li}} &= \sqrt{n_{\mathrm{li}}} \cdot l_{\mathrm{li}} = \sqrt{230} \cdot 2.5\,\text{Å} = 38\,\text{Å} \\ good\ solvent : Rg_{\mathrm{li}} &= (n_{\mathrm{li}})^{3/5} \cdot l_{\mathrm{li}} = (230)^{3/5} \cdot 1.9\,\text{Å} = 50\,\text{Å} \end{aligned} \tag{B.8}$$

The lPEI and bPEI have similar Rg of 4 nm (θ solvent, 5 nm to 6 nm for good solvent). Since lPEI has less segments, it has a higher density than bPEI.